Environment Canada | Environnement Canada

Application of Direct Measurements of Optical Parameters to the Estimation of Lake Water Quality Indicators

R.P. Bukata, J.E. Bruton and J.H. Jerome

SCIENTIFIC SERIES NO. 140

INLAND WATERS DIRECTORATE
NATIONAL WATER RESEARCH INSTITUTE
CANADA CENTRE FOR INLAND WATERS
BURLINGTON, ONTARIO, 1985

(Disponible en français sur demande)

Environment Canada Environnement Canada

Application of Direct Measurements of Optical Parameters to the Estimation of Lake Water Quality Indicators

R.P. Bukata, J.E. Bruton and J.H. Jerome

SCIENTIFIC SERIES NO. 140

INLAND WATERS DIRECTORATE
NATIONAL WATER RESEARCH INSTITUTE
CANADA CENTRE FOR INLAND WATERS
BURLINGTON, ONTARIO, 1985

(Disponible en français sur demande)

Cat. No. En 36-502/140E

ISBN 0-662-14184-9

Contents

Table

Illustrations

Illustrations (Cont.)

Illustrations (Cont.)

Illustrations (Cont.)

Abstract

This report contains an evaluation of direct measurements of optical parameters as a means of estimating water quality indicators (concentrations of chlorophyll *a*, suspended minerals, and dissolved organic carbon) that define natural lake waters. The analyses and discussions presented are based on the results of a coordinated optical/water quality study of a complex inland lake (Lake Ontario), and consequently represent a possible "worst case" approach to the problem, since a body of water such as Lake Ontario would understandably present a severe test of such optical modelling.

The report is not intended as a short course in lake optics, although the necessary mathematical theory is briefly presented, as is a glossary of the technical terminology used in the text. The key linkages between measured optical properties and water quality indicators are the specific absorption and scattering properties (cross sections) of the various aquatic components as a function of observed wavelengths. Considerable discussion is presented concerning not only the techniques used to estimate such optical cross sections but also the departures from constancy of such cross sections for Lake Ontario waters (and waters on a more global scale) and the restrictions that such departures from constancy impose upon water quality prediction.

In its most simple form the method of using optical parameters to estimate water quality considered in this report may be stated as follows: a direct measurement of the subsurface irradiance reflectance (volume reflectance) spectrum is obtained in the 400- to 700-nm (visible) range. Values of the wavelength dependencies of the optical cross sections of chlorophyll, suspended minerals, and dissolved organic carbon are then utilized in conjunction with appropriate optimization methodology to estimate the concentrations of chlorophyll, suspended minerals, and dissolved organic carbon that will generate a subsurface irradiance reflectance spectrum that most closely simulates the directly measured spectrum.

To illustrate the impact on the observed subsurface irradiance reflectance spectrum of varying the concentrations of the three principal organic and inorganic components, the report includes numerous examples of calculated optical spectra for water masses of distinctly dissimilar water quality.

The use of a volume reflectance measurement at a single wavelength as a means of estimating water quality indicators for multi-component waters is all but eliminated by this report. Employing the entire volume reflectance spectrum to estimate water quality indicators, however, appears to be considerably more promising. Despite the severe limitations on predictive capabilities resulting from the inconstancies of the optical cross sections, this work has realized acceptable success in estimating suspended mineral and dissolved organic carbon concentrations in Lake Ontario. This augures well for the use of such predictive methodology in optically less complex inland waters. Reliable predictive capabilities for chlorophyll concentrations continue to be much more elusive.

The model development and application presented here can by no means be regarded as definitive, representing as it does the current level of understanding and state of the art of such aquatic studies. Comparable work, however, is continuing at numerous optically oriented research institutions around the world.

Résumé

Le rapport porte sur l'évaluation des mesures directes de paramètres optiques comme moyens d'estimer les indicateurs (concentrations de chlorophylle *a*, de minéraux en suspension et de carbone organique dissous) de la qualité des eaux lacustres. Les analyses et les discussions présentées se fondent sur les résultats d'une étude par voie optique de la qualité des eaux d'un lac complexe (lac Ontario) et portent donc sur le pire cas possible, une masse d'eau telle que le lac Ontario présentant, on le comprendra, une épreuve très sévère d'une telle modélisation optique.

Le rapport n'est pas destiné à servir de cours abrégé sur l'optique lacustre, même si on présente rapidement la théorie mathématique nécessaire, ainsi qu'un vocabulaire des termes techniques utilisés. Les relations fondamentales entre les propriétés optiques mesurées et les indicateurs de qualité de l'eau sont les propriétés spécifiques d'absorption et de dispersion (selon les sections) des divers éléments du milieu aquatique en fonction des longueurs d'ondes observées. On discute longuement, non seulement des techniques utilisées pour estimer ces sections optiques, mais aussi les anomalies présentées par les eaux du lac Ontario (et les eaux sur une échelle plus générale) ainsi que les restrictions que ces anomalies imposent sur la prévision de la qualité de l'eau.

La méthode optique d'estimation de la qualité de l'eau peut être exposée le plus simplement possible comme suit : on obtient, dans la gamme du visible (400 à 700 nm) et par mesure directe, le spectre de la réflectance de l'irradiation sous la surface (réflectance volumique). Les relations données aux diverses longueurs d'ondes par les sections optiques des eaux chargées de chlorophylle, de minéraux en suspension et de carbone organique dissous servent ensuite, avec l'apport des méthodes appropriées d'optimisation, à estimer la concentration de ces paramètres qui produiront le spectre le plus fidèle au spectre observé.

Pour montrer l'effet de la variation des concentrations sur le spectre observé, le rapport donne de nombreux exemples des spectres optiques calculés pour des masses d'eau dont la qualité diffère de façon tranchée.

La mesure à une seule longueur d'onde est à toutes fins utiles rejetée comme moyen d'estimer les indicateurs de qualité d'une eau complexe. Le recours au spectre entier semble toutefois beaucoup plus prometteur. Les anomalies des sections optiques limitent beaucoup les possibilités de la prédiction, mais notre travail a permis d'estimer de façon acceptable les concentrations de minéraux en suspension et de carbone organique dissous dans le lac Ontario. Ce résultat s'avère de bon augure pour l'application d'une telle méthode de prédiction à des eaux continentales optiquement moins complexes. Quant aux possibilités de prédiction fiable des concentrations de la chlorophylle, elles continuent de nous échapper.

La construction et l'utilisation du modèle présenté ne peuvent en aucun cas être considérées comme définitives, étant le portrait fidèle du niveau actuel des connaissances et des techniques de la discipline. Toutefois, des travaux semblables se poursuivent dans de nombreuses autres institutions de recherche qui, dans le monde, s'intéressent aux paramètres optiques.

Executive Summary

The colour of water has often been considered as an indicator of water quality. This hypothesis is often quantified with a Secchi disk estimate of water transparency and forms the basis for remote airborne or satellite measurements proposed to represent a measure of water quality.

This report examines the basic properties of scattering and absorption of water in terms of three indicators often used as a measure of water quality—concentrations of chlorophyll *a*, suspended minerals, and dissolved organic carbon—and relates these properties to measurable subsurface irradiance reflectance (volume reflectance). The wavelength dependency of each of the water quality indicators is examined, and the interactive influence on the total volume reflectance calculated.

The theoretical considerations indicate that no single wavelength or simple multiple of wavelengths can be used with significant sensitivity to relate the water quality indicators to volume reflectance. If a comprehensive analysis of the entire visible spectrum is considered, the suspended minerals and dissolved organic carbon concentrations may be specified to within a factor of two. In inland lake waters, the specification of chlorophyll *a* concentrations may be extremely hazardous, and in the presence of significant concentrations of suspended minerals and/or dissolved organic carbon, chlorophyll *a* cannot be accurately quantified.

Empirical comparisons of measurements of chlorophyll *a*, suspended minerals, and dissolved organic carbon coincident with measurements of volume reflectance in Lake Ontario were used to validate the theoretical model. In general, reasonable agreements were obtained, with the exception of chlorophyll *a*, where the measured concentrations were generally less than those calculated from the model. Empirical adjustments were able to improve the agreement but indicate that relationships may be inconstant. This problem may relate, at least in part, to the standard methods of measuring chlorophyll *a* and to the relationship of chlorophyll *a* to phytoplankton biomass.

The report provides a thorough examination of the basis and potential of optical measurements to the general area of water quality using the primary property of volume reflectance. This must relate to any airborne or satellite observations.

Application of Direct Measurements of Optical Parameters to the Estimation of Lake Water Quality Indicators

R.P. Bukata, J.E. Bruton and J.H. Jerome

INTRODUCTORY THEORY

The combined processes of scattering and absorption control the manner in which impinging radiation propagates through a natural water mass. The nature and magnitude of the scattering and absorption processes depend, in turn, upon the nature and concentrations of the suspended and dissolved organic and inorganic materials distributed within the water column, as well as on the nature and radiance distribution of the impinging radiation. Since water masses display both spatial and temporal variations in their organic and inorganic compositions, it logically follows that they will be characterized by related variabilities in their observed interactions with the impinging radiation field. Consequently, studies of the optical properties of water masses must contend with two broad categories of optical properties.The *inherent* optical properties of a water mass are those that are totally independent of the spatial distribution of the impinging radiation, while the so-called *apparent* optical properties of a water mass are those that are dependent upon the spatial distribution of impinging radiation.

The apparent optical properties of a water mass include the following:

(a) Irradiance reflectance (volume reflectance), R

(b) Irradiance attenuation coefficient, K.

The inherent optical properties of a water mass include the following:

(a) Total attenuation coefficient, c

(b) Absorption coefficient, a

(c) Scattering albedo, ω_o

(d) Scattering coefficient, b

(e) Forwardscattering probability, F

(f) Backscattering probability, B

(g) Volume scattering function, $\beta(\Theta)$.

The Appendix contains a glossary of technical definitions of the terms used in this report.

Since the electromagnetic frequency spectrum comprises many orders of magnitude, and since water quality is a highly subjective term encompassing myriad species and subspecies of organic and inorganic materials, a comprehensive document relating optical behaviour to water quality is beyond the scope of current capabilities. Consequently, this work will consider as its terms of reference an electromagnetic spectrum restricted to the visible wavelengths (400 to 700 nm) and the quality of a water mass to be defined in terms of its chlorophyll *a*, suspended mineral, and dissolved organic carbon concentrations.

The inherent optical properties b and B are mathematically defined in terms of appropriate integrations of the volume scattering function, $\beta(\Theta)$. Consequently, direct measurements of the inherent optical properties of natural waters require sophisticated instrumentation capable of determining the entire volume scattering function, $\beta(\Theta)$, to separate the scattering coefficient, b, and the absorption coefficient, a, from the total attenuation coefficient, c ($c = a + b$). It is considerably easier, however, to perform *in situ* measurements of the apparent optical properties of the water column. The total attenuation coefficient, c, is readily obtained from transmissometry, and the apparent optical properties, R and K, are readily determined from upwelling and downwelling spectrometric measurements. Consequently, a widely used approach to the general area of ocean and lake optics has been to determine the general relationships between the inherent and apparent optical properties through the development of models based on suitable simulations of the radiative transfer equations. Two such models have been proposed: one by Gordon *et al.* (1975), using a Monte Carlo simulation, and the other by Di Toro (1978), using a combination of an exponential and a quasi-single scattering approximation. Although both radiative transfer simulations have been employed at the National Water Research Institute, the rest of this report will consider only the Gordon *et al.* (1975) simulation.

From Gordon *et al.* (1975), curve fitting to the Monte Carlo calculations results in the equations

$$\omega_o F = \sum_{n=0}^{N} k'_n(\tau) \left[\frac{K(\tau)}{c(\tau)D_d(\tau)}\right]^n \quad (1)$$

and

$$\frac{\omega_o B}{1-\omega_o F} = \sum_{n=0}^{N} r'_n(\tau) [R(\tau)]^n \quad (2)$$

where $\omega_o = \frac{b}{c} \equiv$ scattering albedo

$F \equiv$ forwardscattering probability

$B \equiv$ backscattering probability $= 1-F$

$K(\tau) \equiv$ irradiance attenuation coefficient at depth τ for downwelling irradiance

$R(\tau) \equiv$ irradiance reflectance (volume reflectance) at depth τ for downwelling irradiance

$D_d(\tau) \equiv$ distribution function at depth τ for downwelling irradiance

$c(\tau) \equiv$ total attenuation coefficient at depth τ

$k'_n(\tau)$ and $r'_n(\tau)$ are the sets of appropriate coefficients for the expansions of Equations 1 and 2.

Gordon *et al.* (1975) have determined two sets of values for the coefficients $r'_n(\tau)$, one set appropriate for conditions of solar incidence angles $\lesssim 20°$, and the other set appropriate for solar incidence angles $\gtrsim 30°$ as measured in the water column. The set of coefficients $k'_n(\tau)$ is independent of sun angle.

Equations 1 and 2 then enable the apparent optical properties $K(\tau)$, $R(\tau)$ and the inherent optical property $c(\tau)$ (determined from *in situ* lake measurements) to be used in the determination of the inherent optical properties, ω_o, a, b, F and B. The implicit wavelength dependence of Equations 1 and 2 has been omitted for simplicity.

The inherent optical properties are themselves interrelated ($c = a + b$) and display additive properties which are dependent upon the presence of scattering and absorption centres within the water column:

$$a(\lambda) = \sum_{i=1}^{n} x_i a_i(\lambda)$$

$$b(\lambda) = \sum_{i=1}^{n} x_i b_i(\lambda) \quad (3)$$

$$(Bb)(\lambda) = \sum_{i=1}^{n} x_i (Bb)_i(\lambda)$$

where $(Bb)(\lambda) \equiv$ backscatter coefficient at wavelength λ, the product of B and b

$x_i \equiv$ concentration of the ith component of the water mass in question

$a_i(\lambda) \equiv$ absorption at wavelength λ for a unit concentration of component i

$b_i(\lambda) \equiv$ scattering at wavelength λ for a unit concentration of component i

$(Bb)_i(\lambda) \equiv$ backscattering at wavelength λ for a unit concentration of component i.

Since $a_i(\lambda)$, $b_i(\lambda)$ and $(Bb)_i(\lambda)$ represent the optical behaviour (in terms of absorption and scattering) of the water column per unit concentration of component matter, they will be referred to as the optical cross sections of the water mass in subsequent discussions. The determination of these optical cross sections clearly provides the linkages between the inherent optical properties of a water mass and its water quality parameters. Obviously, the definitive optical model should consider the cross sections of every species and subspecies of aquatic components present in natural water masses, as well as possible temporal, shape and size dependencies of each. Such a model is clearly unattainable. The present work considers that at any instant of time a natural water mass may be taken to be defined by a homogeneous combination of pure water, unique suspended organic material (considered to be represented by the chlorophyll *a* concentration corrected for phaeophytin contamination), unique suspended inorganic material (considered to be represented by the suspended mineral concentration, SM), dissolved organic material (represented by dissolved organic carbon, DOC) and a non-living organic component NLO, determined in the following manner:

$$\frac{NLO}{78} = \frac{SO}{78} - \frac{Chl_{cor}}{Chl_{unc}} \cdot \frac{POC}{24} \quad (4)$$

where SO = measured value of total suspended organic material concentration

Chl_{unc} = measured value of chlorophyll *a* uncorrected for phaeophytin contamination

Chl_{cor} = measured value of chlorophyll *a* corrected for phaeophytin contamination

POC = measured value of particulate organic carbon concentration.

The units in Equation 4 have been normalized on the assumption (Burns, 1980) that the average organic component may be represented by the molecular formula $C_2H_6O_3$ (and therefore by a molecular weight of 78 a.u.). Equation 4, however, does not take into account the contribution from the living zooplankton population.

For such a five-component optical model (SM, Chl *a*, DOC, NLO, plus pure water), Equation set 3 may be written

$$a(\lambda) = a_w(\lambda) + xa_{Chl}(\lambda) + ya_{SM}(\lambda) + za_{DOC}(\lambda) + u\,a_{NLO}(\lambda)$$

$$b(\lambda) = b_w(\lambda) + x\,b_{Chl}(\lambda) + y\,b_{SM}(\lambda) + u\,b_{NLO}(\lambda) \quad (5)$$

$$(Bb)(\lambda) = (Bb)_w(\lambda) + x(Bb)_{Chl}(\lambda) + y(Bb)_{SM}(\lambda) + u(Bb)_{NLO}(\lambda)$$

where the subscripts w, Chl, SM, DOC and NLO refer to the pure water, unique organic, unique inorganic, dissolved organic and unique non-living organic components of the water column, respectively; x, y, z and u are the concentrations of chlorophyll *a* (corrected for phaeophytin contamination), suspended minerals, dissolved organic carbon, and non-living organic material, respectively; and the components of a (a_{Chl}, a_{SM}, a_{DOC}, a_{NLO}), b(b_{Chl}, b_{SM}, b_{NLO}) and Bb[$(Bb)_{Chl}$, $(Bb)_{SM}$, $(Bb)_{NLO}$] are the optical cross sections.

To obtain values for the cross sections, a coordinated spectro-optical program was conducted in western Lake Ontario. The entire program was a joint venture between NWRI (National Water Research Institute), CCRS (Canada Centre for Remote Sensing) and Moniteq Ltd., which included an airborne remote sensing and atmospheric study component in addition to the *in situ*/theoretical optical program discussed in this report. Logistical details of the multi-stage Lake Ontario experiment are presented elsewhere (Jain *et al.*,1980; Zwick *et al.*, 1980; Bukata *et al.*, 1981a,b). Suffice to say that coordinated collections of water samples (which were laboratory-analyzed for water quality parameters) occurred in conjunction with *in situ* determinations of transmission profiles (using a modified Martek multiband XMS transmissometer) and spectral irradiance profiles and spectral volume reflectance (using a Techtum QSM 2500 scanning Quanta spectrometer) in the upper 10 m of water. Details of the numerical determinations of the optical cross sections are given in Bukata *et al.* (1981a). The flow diagram of Figure 1 outlines the basic steps taken. The *in situ* transmissometer and spectrometer data were used to determine the inherent optical property, $c(\lambda,\tau)$, and the apparent optical properties, $K(\lambda,\tau)$ and $R(\lambda,\tau)$. The Gordon *et al.* (1975) model (Equations 1 and

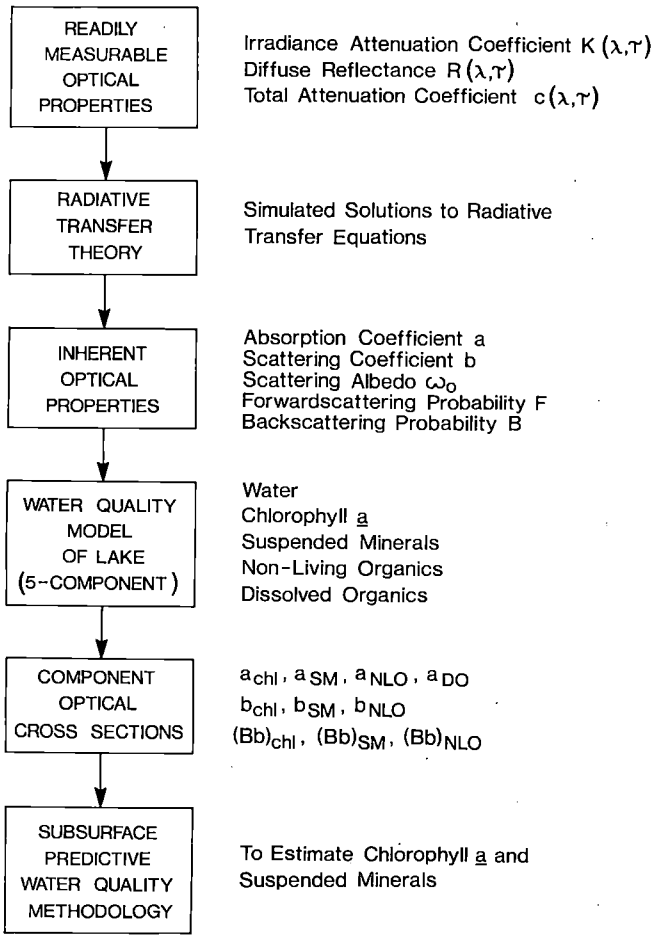

Figure 1. Flow diagram outlining the operations employed in the development of subsurface optical water quality methodology.

2) was utilized (see Bukata *et al.*, 1979) to determine the inherent optical properties a, b, ω_o, F and B. Multiple regression techniques applied to the determined values of a, b and (Bb) and the measured values of water quality parameters (Equation set 5) yielded the desired optical cross sections for the five-component model.

It was discovered, however, at least for Lake Ontario, that only a slight loss in generality occurred when a four-component optical model that disregarded the contribution of NLO was considered. This was partly because the NLO component was rarely a dominant factor in the optical behaviour of Lake Ontario (the numerical value of NLO concentration [in grams per cubic metre] rarely exceeded 10% of the numerical value of chlorophyll *a* concentration [in milligrams per cubic metre]). However, the use of a four-component model necessitated the use of Chl a_{unc} (i.e., chlorophyll *a* concentration uncorrected for phaeophytin contamination). Consequently, the rest of this report will deal with a four-component optical model (pure water, chlorophyll *a* with phaeophytin, suspended minerals, and dissolved organic carbon). In such a model, Equation set 5 becomes:

$$a(\lambda) = a_w(\lambda) + xa_{Chl}(\lambda) + ya_{SM}(\lambda) + za_{DOC}(\lambda)$$

$$b(\lambda) = b_w(\lambda) + xb_{Chl}(\lambda) + yb_{SM}(\lambda) \qquad (6)$$

$$(Bb)(\lambda) = (Bb)_w(\lambda) + x(Bb)_{Chl}(\lambda) + y(Bb)_{SM}(\lambda)$$

where it is noted that the subscript Chl now refers to Chl a_{unc} and x refers to the concentration of Chl a_{unc}.

OPTICAL CROSS SECTIONS FOR LAKE ONTARIO

The cross sections for the four-component optical model (pure water, SM, Chl a_{unc}, DOC) are illustrated in Figures 2 and 3 as a function of visible wavelength. Figure 2 illustrates the $a_i(\lambda)$ values and Figure 3 illustrates the $b_i(\lambda)$ values for Lake Ontario waters. The values of $a_w(\lambda)$ and $b_w(\lambda)$ were taken from the work of Hulburt (1945). Once these optical cross sections are known, a volume reflectance spectrum $R_v(\lambda)$ may be generated for water masses made up of varying amounts of chlorophyll *a* (uncorrected for phaeophytin contamination), suspended minerals, and dissolved organic carbon, utilizing the Gordon *et al.* (1975) Monte Carlo simulation model. Therefore in principle, *in situ* measured volume reflectance spectra could be compared with a catalog of existing volume reflectance spectra for water masses made up of known component concentrations. Such comparison, however, is subject to the following stipulations:

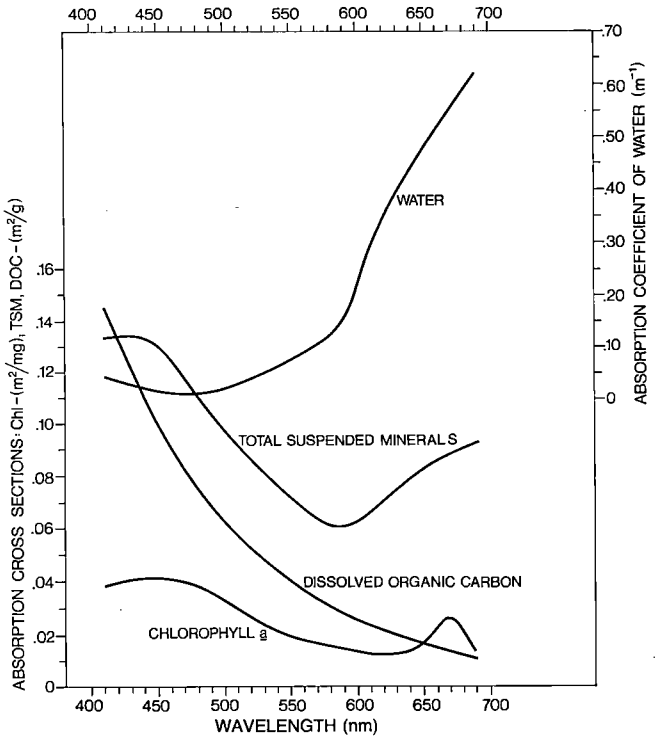

Figure 2. The calculated absorption cross sections for chlorophyll *a* uncorrected for phaeophytin contamination (Chl a_{unc}), total suspended minerals (SM), and dissolved organic carbon (DOC). Also shown are the absorption coefficients for pure water.

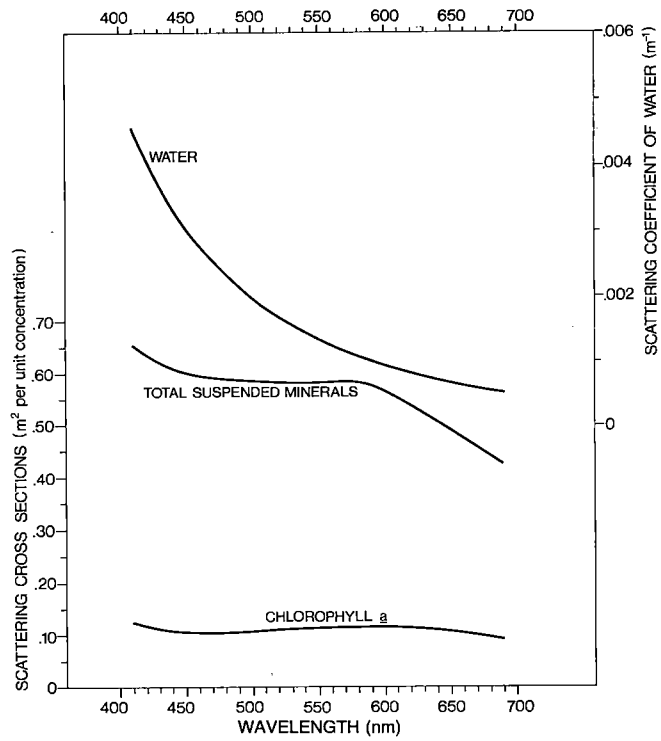

Figure 3. The calculated scattering cross sections for chlorophyll *a* uncorrected for phaeophytin contamination (Chl a_{unc}) and total SM. Also shown are the scattering coefficients for pure water.

(a) The natural waters under consideration must be appropriately defined by a four-component optical model. Clearly, the more optically complex a water mass becomes (i.e., the greater the number of components which significantly alter its optical behaviour), the less reliable will be the use of the current model in providing lake water quality indicators.

(b) The optical cross sections must be known. Furthermore, they must be confidently assumed to be relatively invariant, or at least insignificantly varying during the measurement time interval. Such conditions are satisfied at some locations and time periods but not at others. For example, the optical cross sections determined in western Lake Ontario have been shown to possess, to a large degree, a lake-wide applicability (Bukata *et al.*, 1981c) throughout most of the field season. However, as yet unpublished work appears to indicate that Lake Ontario waters may require an independent set of optical cross sections during the autumn months (due possibly to a change in the indigenous chlorophyll-bearing biota).

(c) The water mass is considered to be homogeneous. The current model does not include possible layering effects.

(d) No provision is incorporated for chemical impurities. Small concentrations of such chemicals (by comparison with the concentrations of Chl, SM and DOC) produce negligible absorption and scattering effects and their detection is beyond current *in situ* optical techniques.

SUBSURFACE IRRADIANCE REFLECTANCE SPECTRA

From Gordon *et al.* (1975), the irradiance reflectance (also referred to as the volume reflectance), $R(0,\lambda)$, just beneath the free-surface layer is given by

$$R(0,\lambda) = \sum_{n=0}^{N} r_n(0) \left[\frac{Bb(\lambda)}{a(\lambda) + Bb(\lambda)}\right]^n \qquad (7)$$

where all terms are as previously defined. The term $r_n(0)$ signifies the expansion coefficients, considered in this work as those appropriate for solar incidence angles $\lesssim 20°$, as measured within the water column. Furthermore, N is taken as 3. Using the additive properties of $a(\lambda)$ and $Bb(\lambda)$ displayed in Equation set 6 for the four-component water mass representation, and using the optical cross sections illustrated in Figures 2 and 3, it is clear that point-by-point subsurface irradiance reflectance spectra may be generated for selected values of x, y and z, i.e., for a variety of water masses displaying varying concentrations of chlorophyll *a* (uncorrected for phaeophytin contamination), suspended minerals, and dissolved organic carbon.

Figure 4 illustrates a family of subsurface irradiance reflectance spectra (at 20-nm increments from 410 to 690 nm) calculated in this manner for varying chlorophyll *a* concentrations in a water mass for which the suspended mineral and dissolved organic carbon concentrations are kept fixed at zero (i.e., for a two-component model of the water mass, namely chlorophyll and pure water). Clearly, water masses with small concentrations of chlorophyll *a* display a pronounced volume reflectance in the blue region of the spectrum and minimal volume reflectance in the red. Increasing the chlorophyll concentration in such a water mass (i.e., a water mass composed solely of pure water and chlorophyll) tends to decrease the volume reflectance at the blue wavelengths while increasing the volume reflectance at the red wavelengths at a more rapid rate. For chlorophyll concentrations of more than ~ 1 to 2 mg m^{-3}, the irradiance reflectance spectra are characterized by well-defined blue minima and green maxima. Of particular note is the pivotal role played by the 505-nm wavelength, indicating that in such waters (i.e., pure water and chlorophyll) the volume reflectance at 505-nm is independent of the chlorophyll concentration, i.e. $\frac{\partial R(0,505)}{\partial Chl} = 0$. By integrating Equation 7 with respect to chlorophyll, it may be shown that the volume reflectance will be independent of chlorophyll at that value of λ for which $\frac{Bb_{Chl}}{a_{Chl}} = \frac{Bb_w}{a_w}$, i.e., at that value of λ for which the backscatter to absorption ratio of chlorophyll is equal to the backscatter to absorption ratio of pure water. Therefore, an equilibrium is established between the optical properties of each of the two aquatic components.

The effect of the insertion of a small fixed concentration of suspended minerals (0.10 g m^{-3}) into the water mass (i.e., a three-component representation) is shown in the family of subsurface irradiance reflectance spectra illustrated in Figure 5. In such a water mass (0.10 g m^{-3} SM, zero DOC), the rate at which the volume reflectance in the blue region is depressed by the addition of chlorophyll is more nearly equal to the rate of elevation of the volume reflectance in the red. The pivotal wavelength at which $\frac{\partial R(0,\lambda)}{\partial Chl} = 0$ has shifted to ~ 570 nm. For such a three-component water mass representation (pure water, chlorophyll and suspended minerals), the volume reflectance will be independent of chlorophyll concentration at that wavelength for which $\frac{Bb_{Chl}}{a_{Chl}} = \frac{Bb_w + Bb_{SM}C_{SM}}{a_w + a_{SM}C_{SM}}$.

An equilibrium is thus established between the optical properties of chlorophyll and the combined optical properties of the remaining two aquatic components.

In a similar manner, Figures 6 to 12 represent the family of subsurface irradiance reflectance spectra for varying chlorophyll concentrations, a fixed concentration of zero DOC, and fixed suspended mineral concentrations of 0.2, 0.5, 1.0, 2.0, 5.0, 10.0 and 20.0 g m^{-3}, respectively. Note that the pivotal wavelength at which $\frac{\partial R(0,\lambda)}{\partial Chl} = 0$ rapidly moves beyond 690 nm as the suspended mineral concentration increases.

Even though the dramatic impact upon the subsurface irradiance reflectance spectrum of adding suspended mineral concentrations to a lake containing chlorophyll may be readily appreciated from a consideration of Figures 4 to 12, Figure 13 illustrates the evaluation of subsurface irradiance reflectance spectra resulting from a systematic increase of suspended mineral concentration in a lake containing zero DOC and a small fixed amount of chlorophyll. Similarly, Figure 14 illustrates the effect of varying suspended mineral concentrations in a lake containing zero DOC and a large fixed amount of chlorophyll. As logically expected, large concentrations of suspended minerals (say of more than ~ 0.5 g m^{-3}) drastically curtail the spectral sensitivity of the volume reflectance to changes in chlorophyll concentrations.

Clearly, therefore, a wide range of subsurface irradiance reflectance spectra may be anticipated for a three-component (pure water, chlorophyll, suspended minerals) representation of a water mass. The addition of a fourth component (DOC) to the lake system will also significantly alter the irradiance reflectance spectrum observed just beneath the air/water interface, particularly at the lower visible wavelengths (Fig. 2). This impact is readily seen in Figure 15 for the family of volume reflectance spectra (for varying DOC concentrations) for a water mass with a small fixed suspended mineral concentration of 0.05 g m^{-3} and a fixed chlorophyll *a* concentration of 1.00 mg m^{-3}. It is evident that for relatively clear waters (i.e., waters characterized by small concentrations of suspended minerals and small to moderate concentrations of chlorophyll), the systematic addition of DOC results in a rapid depression of the subsurface irradiance reflectance at wavelengths of less than ~600 nm (i.e., the blue and green region of the visible spectrum), and a comparatively minimal depression of the subsurface irradiance reflectance at wavelengths of more than ~ 600 nm (i.e., in the red region of the visible spectrum).

Figure 16 illustrates the impact of DOC on a water mass characterized by a large fixed concentration of Chl *a* (10.0 mg m^{-3}) and a small fixed concentration of suspended minerals (0.05 g m^{-3}), whereas Figure 17 illustrates the impact of DOC on a water mass characterized by a small fixed concentration of Chl *a* (0.05 mg m^{-3}) and a large fixed concentration of suspended minerals (10.0 g m^{-3}). For the water masses depicted in Figures 16 and 17, it is clear that

(a) The water mass containing high concentrations of suspended minerals displays volume reflectance spectra which are an order of magnitude higher than the water mass containing high concentrations of chlorophyll.

(b) The effect of DOC is more noticeable in water masses containing high chlorophyll and low suspended mineral concentrations than in water masses containing low chlorophyll and high suspended mineral concentrations.

(c) For all water masses, the maximum impact of DOC will be registered in the low-wavelength (blue) portion of the visible spectrum, while the minimum impact of DOC will be registered in the high-wavelength (red) portion of the visible spectrum.

Although local values of DOC may vary, both spatially and temporally throughout inland aquatic systems, it has been observed (Bukata *et al.*, 1981a) that a not unreasonable typical value for the dissolved organic carbon concentration for the lower Great Lakes is ~ 2.0 g carbon m^{-3}. Figures 18 and 19 illustrate the anticipated changes in subsurface irradiance reflectance spectra resulting from changes in chlorophyll and suspended mineral concentrations, respectively, in a lake characterized by a fixed DOC concentration of 2.0 g carbon m^{-3}. Figure 18 illustrates the family of volume reflectance spectra produced by varying the chlorophyll concentrations in a water mass containing no suspended mineral concentration, whereas Figure 19 illustrates the family of volume reflectance spectra resulting from varying the suspended mineral concentrations in a water mass containing virtually no chlorophyll (a small fixed concentration of 0.05 mg m^{-3}).

Certain similarities between Figures 18 and 19 are immediately apparent. Increasing either the suspended mineral or chlorophyll concentration in a water mass containing 2.0 g carbon m^{-3} DOC results in more rapid volume reflectance increases in the red end of the spectrum than in the blue, with the basic shape of the spectrum of chlorophyll in the absence of suspended minerals becoming very similar to the basic shape of the spectrum of suspended

minerals in the absence of chlorophyll. Clearly, large concentrations of suspended minerals result in volume reflectance values an order of magnitude greater than those resulting from large concentrations of chlorophyll. Similarly, small concentrations of suspended minerals result in volume reflectance values an order of magnitude greater than those resulting from small concentrations of chlorophyll. However, as seen from Figures 18 and 19, for natural water masses containing 2.0 g carbon m^{-3} DOC, comparable volume reflectance values are observed for water masses containing large concentrations of chlorophyll (and no suspended minerals) and for water masses containing relatively small concentrations of suspended minerals (and no chlorophyll).

The effects on observed subsurface irradiance reflectance spectra of increasing the suspended mineral concentration in a lake containing a fixed DOC concentration of 2.0 g carbon m^{-3} and a large fixed chlorophyll *a* concentration of 10.0 mg m^{-3} are illustrated in Figure 20.

Figure 21 depicts the interactive effects on the volume reflectance spectra of varying both the chlorophyll and the suspended mineral concentrations in a lake containing 2.0 g carbon m^{-3} DOC. Figure 22 illustrates a comparable situation in a lake containing 10.0 g carbon m^{-3} DOC.

Clearly, the examples of subsurface irradiance reflectance spectra presented in this section serve to illustrate the impact that variations in the water quality parameters (chlorophyll, suspended minerals, dissolved organic carbon) will have on the *in situ* measurements of such optical spectra and consequently underline the care that must be taken in deconvolving optical complexities when measured volume reflectance spectra are used to estimate the water quality parameters.

It is equally clear that the examples of subsurface irradiance reflectance spectra presented in this report are inexhaustive, and by no means cover the myriad spectra possible for lakes as complex as Lake Ontario. Consequently, Table 1 contains a numerical listing of the 15-point (20-nm increments from 410 to 690 nm) absorption and backscatter cross-section spectra utilized in this report. The interested reader may use the data in Table 1 together with Equations 6 and 7 to generate the anticipated subsurface irradiance reflectance (volume reflectance) for any desired water mass.

Table 1. Fifteen-Point Absorption and Backscatter Cross-section Spectra Used with Equations 6 and 7 of This Report

Wavelength (nm)	a_w	a^1_{Chl}	a^2_{Chl}	a_{SM}	a_{DOC}	$(Bb)_w$	$(Bb)_{Chl}$	$(Bb)_{SM}$
410	0.038 00	0.037 80	0.024 28	0.133 50	0.145 00	0.002 29	0.001 36	0.052 40
430	0.026 00	0.040 50	0.021 88	0.135 10	0.121 00	0.001 86	0.001 25	0.049 92
450	0.017 00	0.041 00	0.019 38	0.130 90	0.100 00	0.001 52	0.001 19	0.048 16
470	0.017 00	0.040 20	0.018 17	0.116 80	0.082 90	0.001 28	0.001 16	0.047 60
490	0.021 00	0.035 50	0.015 86	0.103 40	0.068 80	0.001 08	0.001 17	0.047 36
510	0.026 00	0.030 40	0.013 41	0.092 20	0.057 00	0.000 91	0.001 20	0.047 12
530	0.030 00	0.023 60	0.008 55	0.083 40	0.048 00	0.000 77	0.001 25	0.046 80
550	0.037 00	0.019 00	0.005 84	0.073 70	0.040 10	0.000 66	0.001 28	0.046 88
570	0.057 00	0.017 30	0.005 50	0.063 80	0.033 30	0.000 58	0.001 27	0.046 96
590	0.112 00	0.015 00	0.002 96	0.061 10	0.027 90	0.000 50	0.001 24	0.046 16
610	0.236 00	0.012 50	0.005 18	0.067 40	0.023 40	0.000 44	0.001 25	0.044 08
630	0.274 00	0.012 00	0.018 14	0.076 60	0.019 50	0.000 38	0.001 22	0.041 60
650	0.303 00	0.016 00	0.022 31	0.083 50	0.016 20	0.000 33	0.001 16	0.039 20
670	0.370 00	0.026 00	0.027 21	0.087 30	0.015 20	0.000 30	0.001 09	0.036 80
690	0.463 00	0.013 00	0.017 16	0.092 70	0.010 50	0.000 26	0.000 99	0.034 08

a^1_{Chl} = The chlorophyll absorption cross section represented by curve B in Figure 46.
a^2_{Chl} = The chlorophyll absorption cross section represented by curve C in Figure 46.

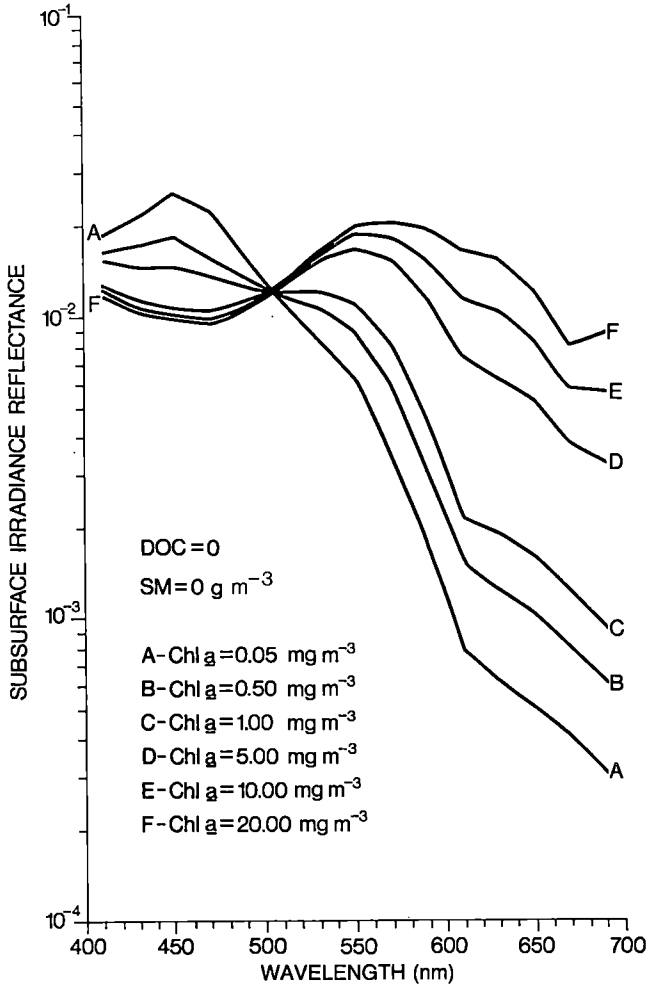

Figure 4. Subsurface irradiance reflectance spectra for various chlorophyll *a* concentrations in a water mass for which the SM and DOC concentrations are kept fixed at zero.

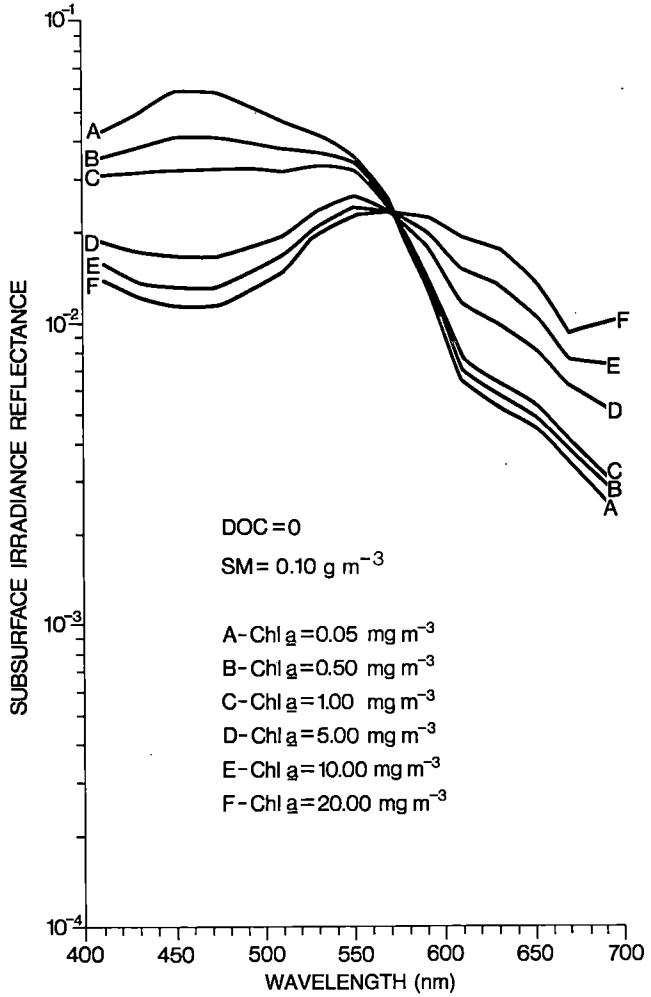

Figure 5. Subsurface irradiance reflectance spectra for various chlorophyll *a* concentrations in a water mass for which the DOC concentration is kept fixed at zero and the total SM concentration, at 0.10 g m^{-3}.

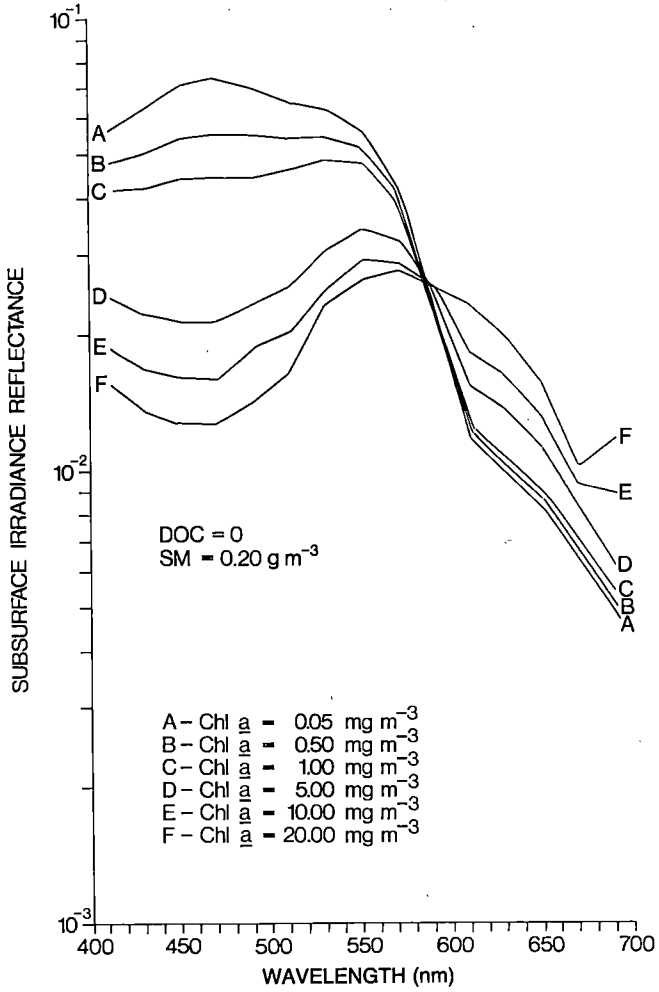

Figure 6. Subsurface irradiance reflectance spectra for various chlorophyll *a* concentrations in a water mass for which the DOC concentration is kept fixed at zero and the total SM concentration, at 0.20 g m^{-3}

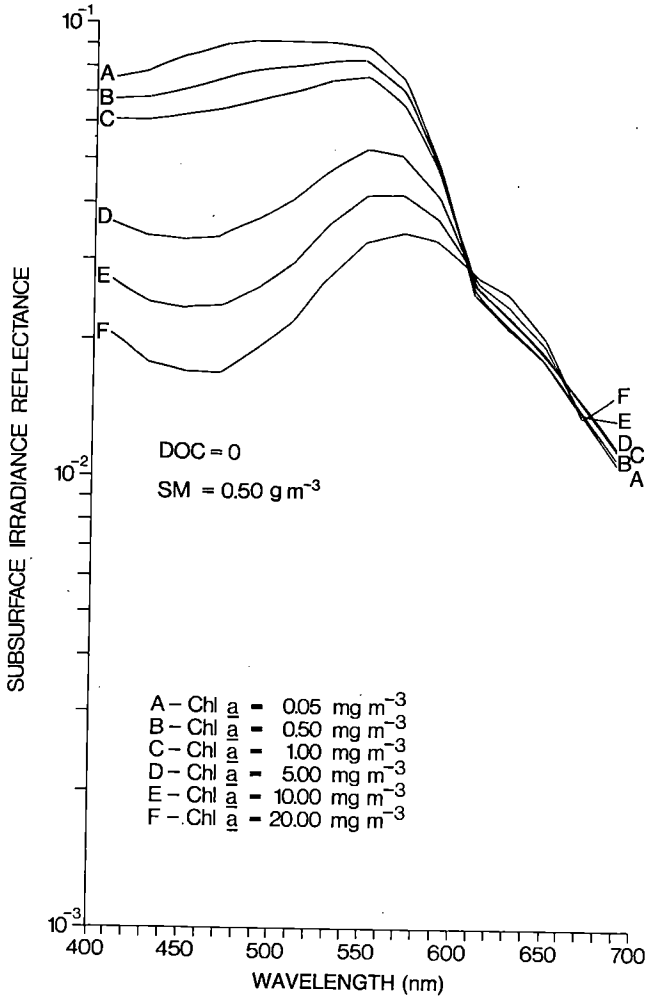

Figure 7. Subsurface irradiance reflectance spectra for various chlorophyll *a* concentrations in a water mass for which the DOC concentration is kept fixed at zero and the total SM concentration, at 0.50 g m^{-3}.

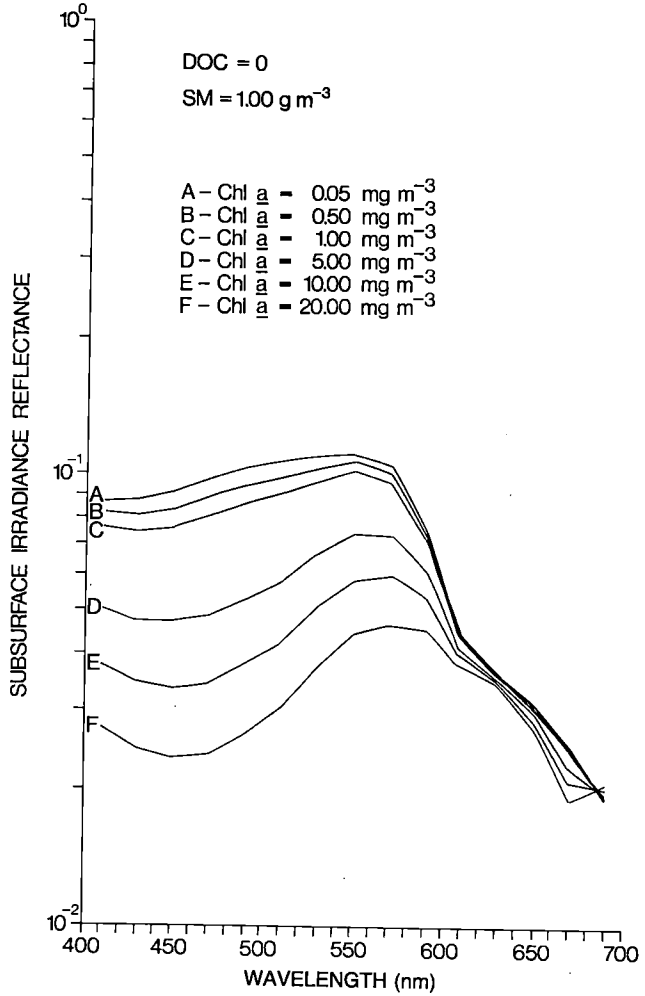

Figure 8. Subsurface irradiance reflectance spectra for various chlorophyll *a* concentrations in a water mass for which the DOC concentration is kept fixed at zero and the total SM concentration, at 1.00 g m^{-3}.

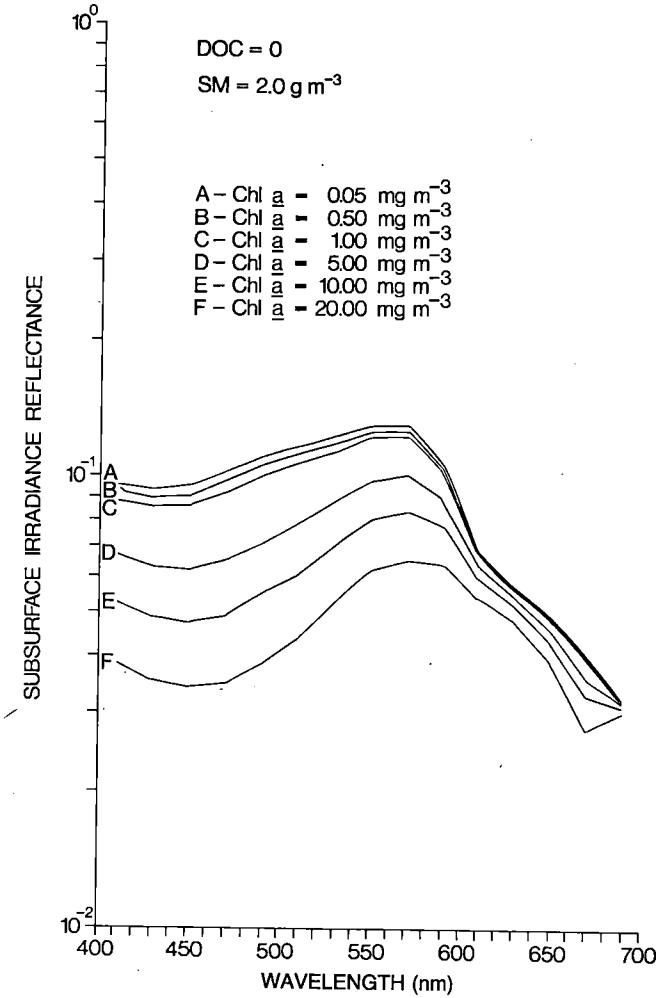

Figure 9. Subsurface irradiance reflectance spectra for various chlorophyll *a* concentrations in a water mass for which the DOC concentration is kept fixed at zero and the total SM concentration, at 2.0 g m^{-3}.

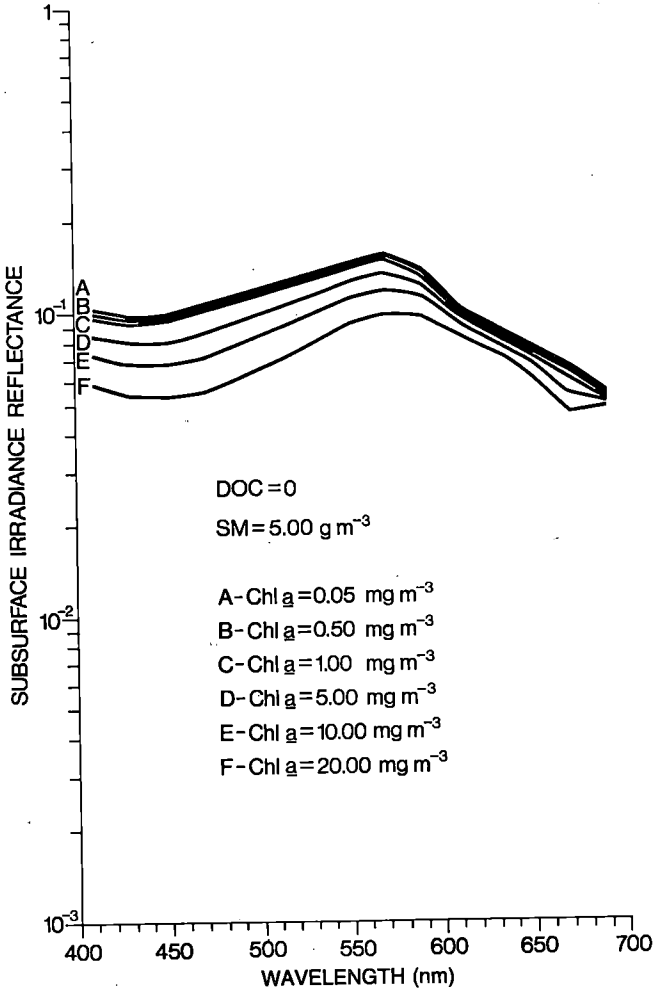

Figure 10. Subsurface irradiance reflectance spectra for various chlorophyll *a* concentrations in a water mass for which the DOC concentration is kept fixed at zero and the total SM concentration, at 5.00 g m^{-3}.

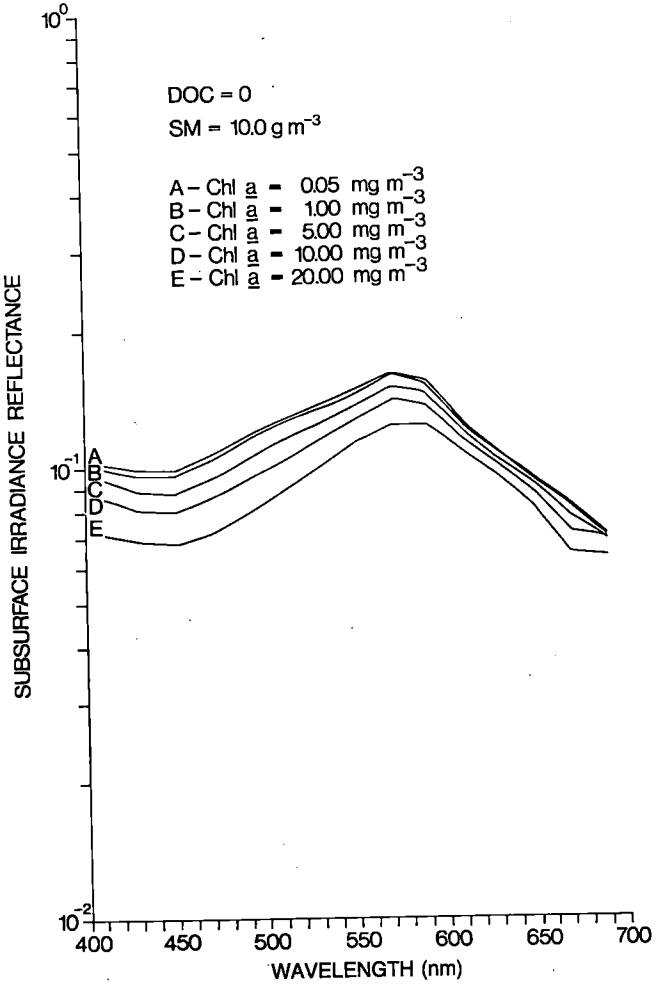

Figure 11. Subsurface irradiance reflectance spectra for various chlorophyll *a* concentrations in a water mass for which the DOC concentration is kept fixed at zero and the total SM concentration, at 10.0 g m^{-3}.

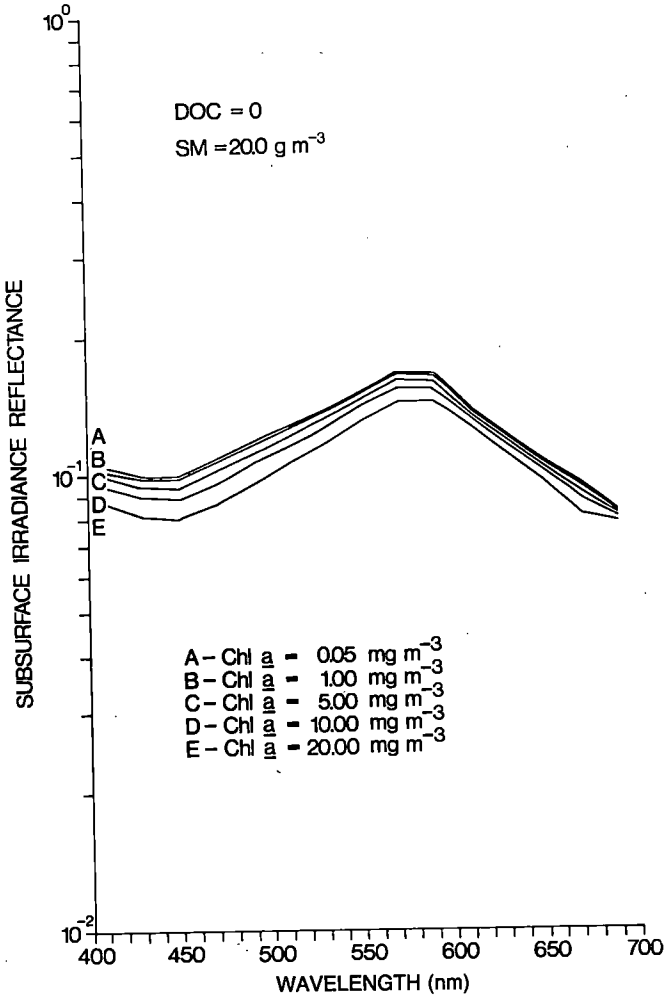

Figure 12. Subsurface irradiance reflectance spectra for various chlorophyll *a* concentrations in a water mass for which the DOC concentration is kept fixed at zero and the total SM concentration, at 20.0 g m^{-3}.

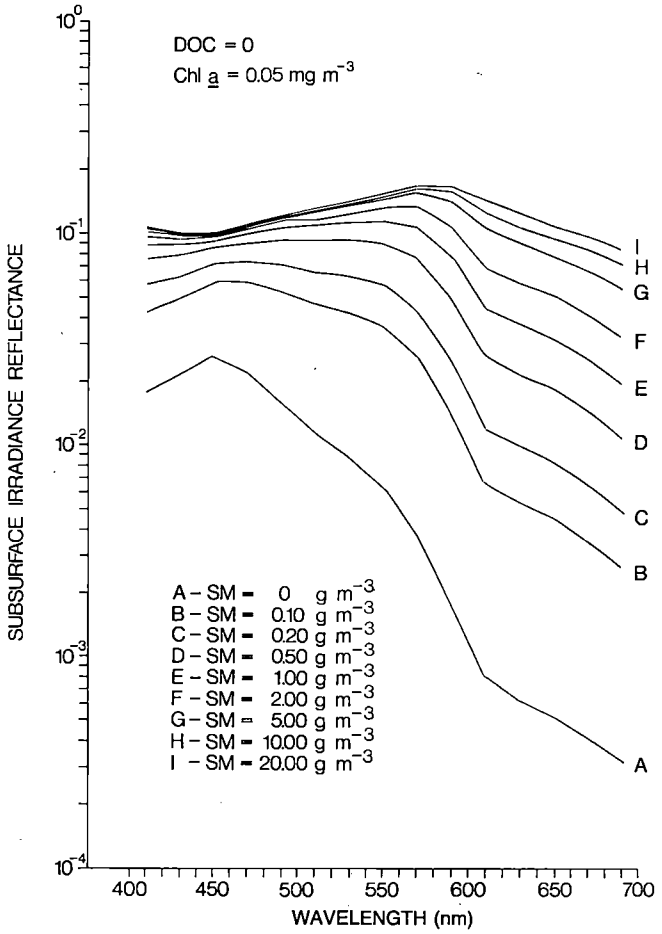

Figure 13. Subsurface irradiance reflectance spectra for various SM concentrations in a water mass containing a small fixed concentration of chlorophyll *a* and zero DOC.

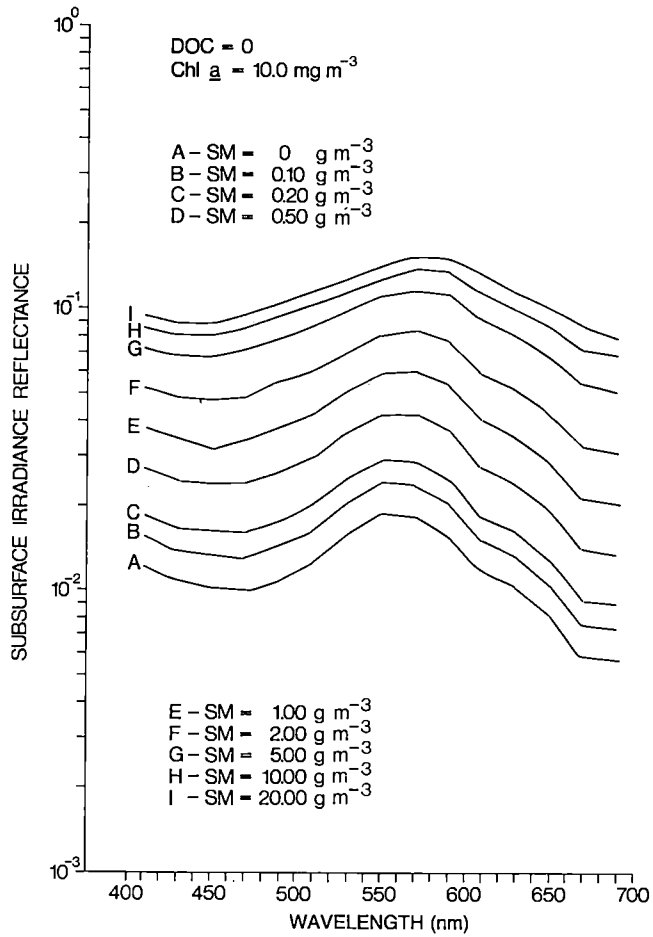

Figure 14. Subsurface irradiance reflectance spectra for various SM concentrations in a water mass containing a large fixed concentration of chlorophyll *a* and zero DOC.

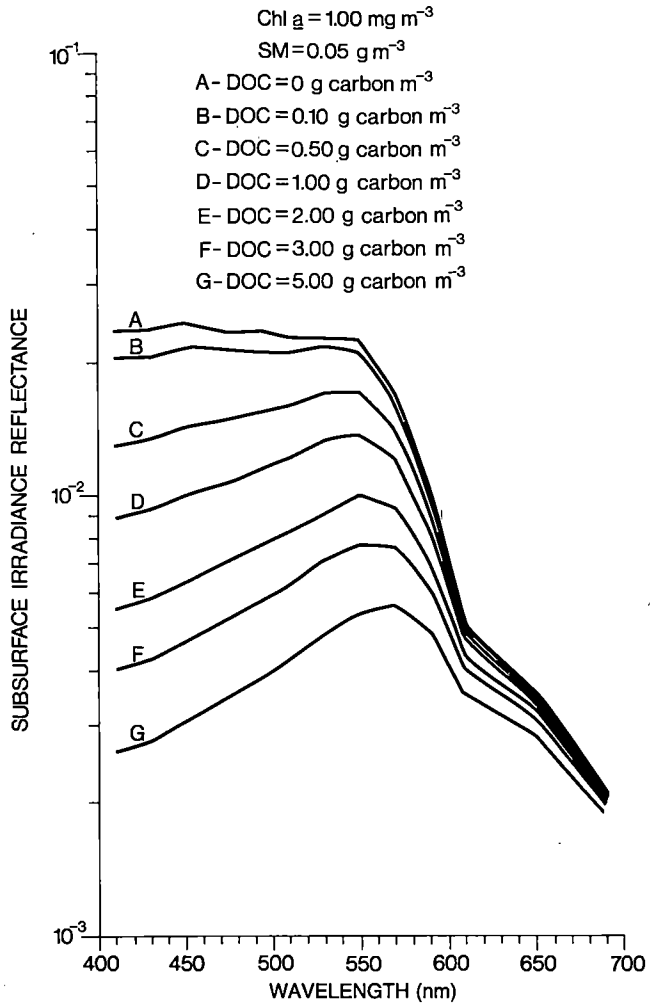

Figure 15. Subsurface irradiance reflectance spectra for various DOC concentrations in a water mass for which the SM concentration is kept fixed at 0.05 g m^{-3} and the chlorophyll *a* concentration, at 1.00 mg m^{-3}.

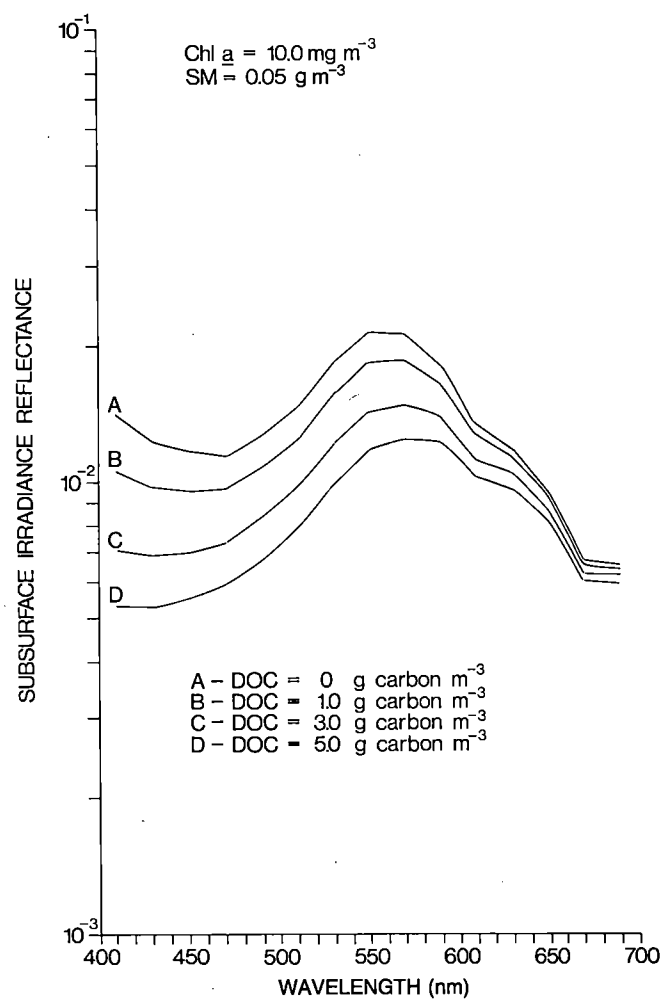

Figure 16. Subsurface irradiance reflectance spectra for various DOC concentrations in a water mass containing a large fixed concentration of chlorophyll *a* (10.0 mg m^{-3}) and a small fixed SM concentration (0.05 g m^{-3}).

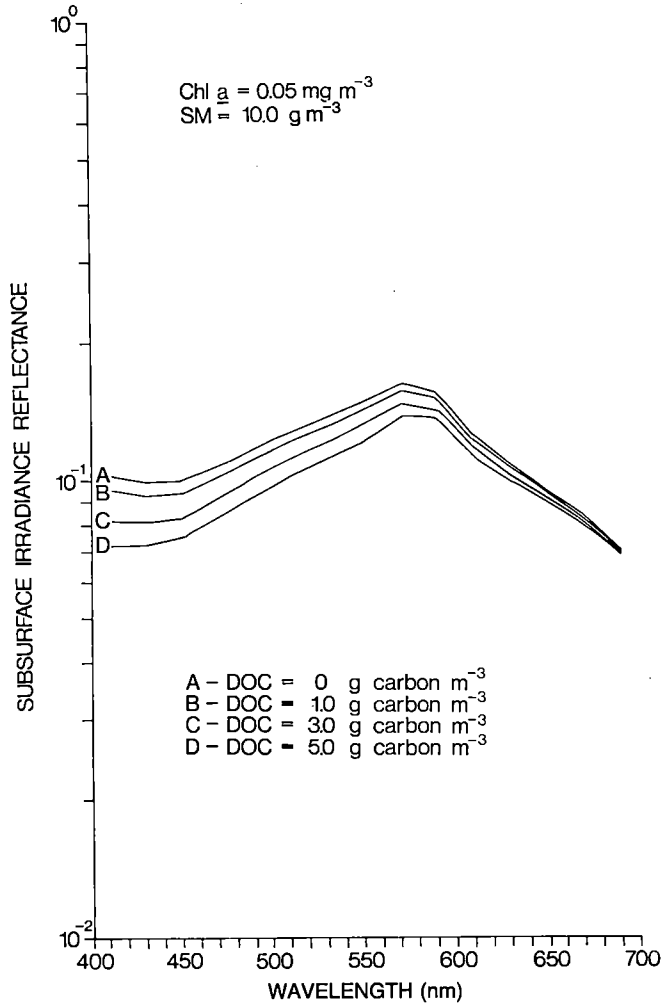

Figure 17. Subsurface irradiance reflectance spectra for various DOC concentrations in a water mass containing a small fixed chlorophyll *a* concentration (0.05 mg m^{-3}) and a large fixed SM concentration (10.0 g m^{-3}).

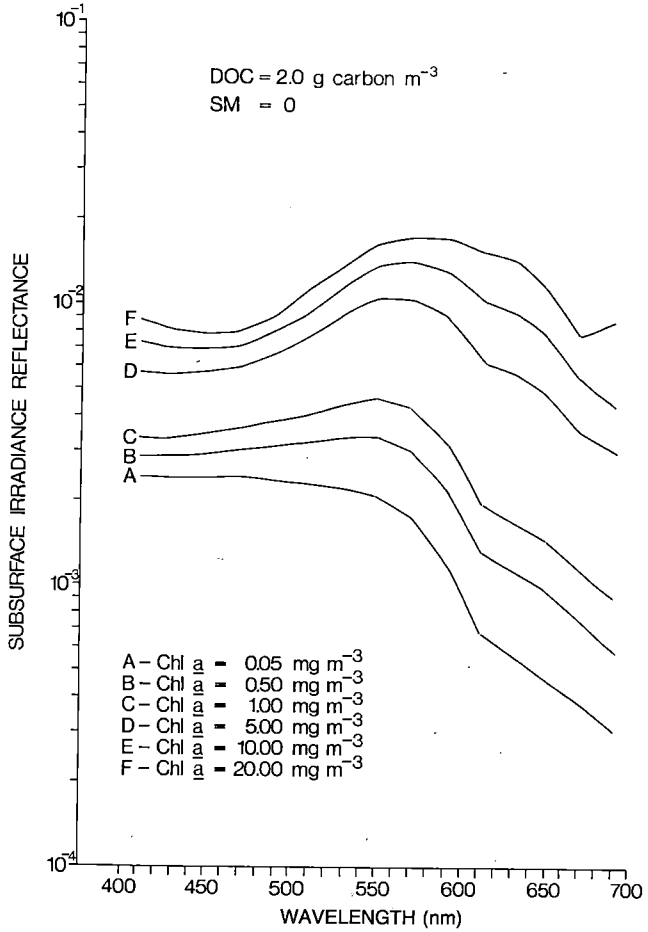

Figure 18. Subsurface irradiance reflectance spectra for various chlorophyll *a* concentrations in a water mass for which the DOC concentration is kept fixed at 2.0 g carbon m^{-3} and the total SM concentration, at zero.

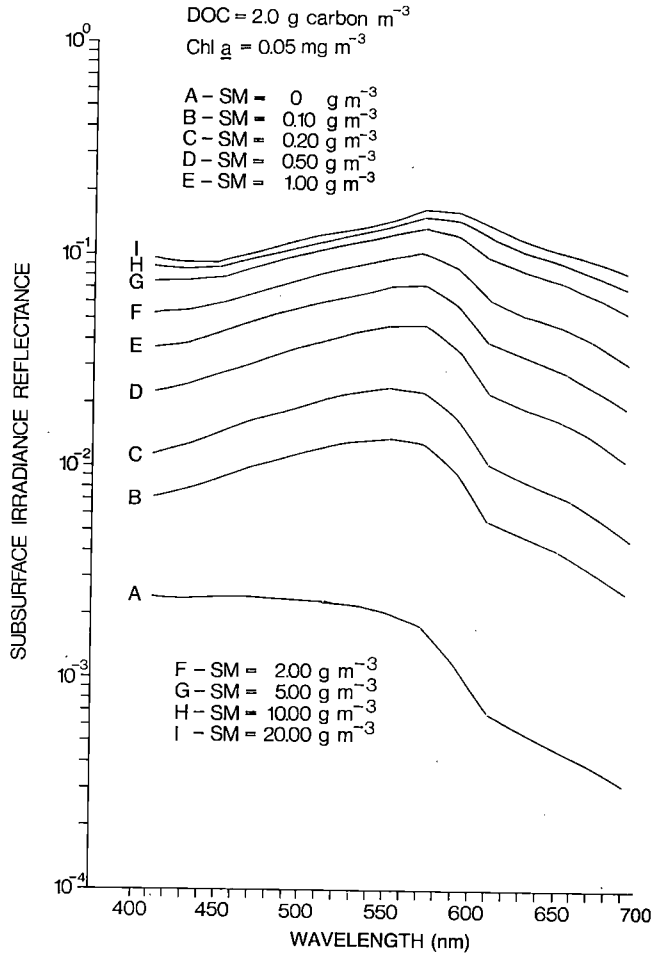

Figure 19. Subsurface irradiance reflectance spectra for various SM concentrations in a water mass for which the DOC concentration is kept fixed at 2.0 g carbon m^{-3} and the chlorophyll *a* concentration, at 0.05 mg m^{-3}.

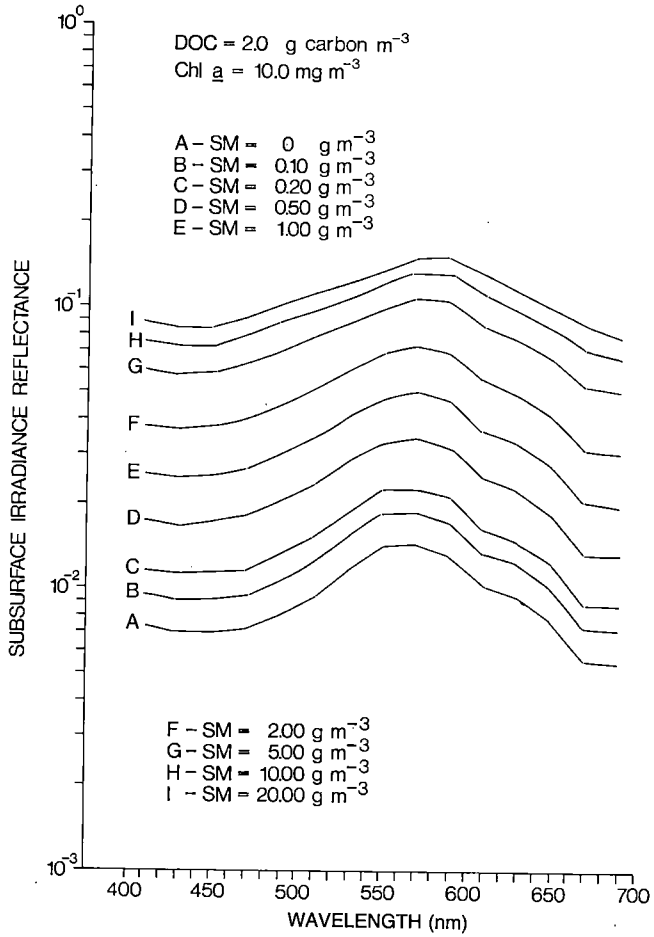

Figure 20. Subsurface irradiance reflectance spectra for various SM concentrations in a water mass for which the DOC concentration is kept fixed at 2.0 g carbon m^{-3} and the chlorophyll *a* concentration, at 10.0 mg m^{-3}.

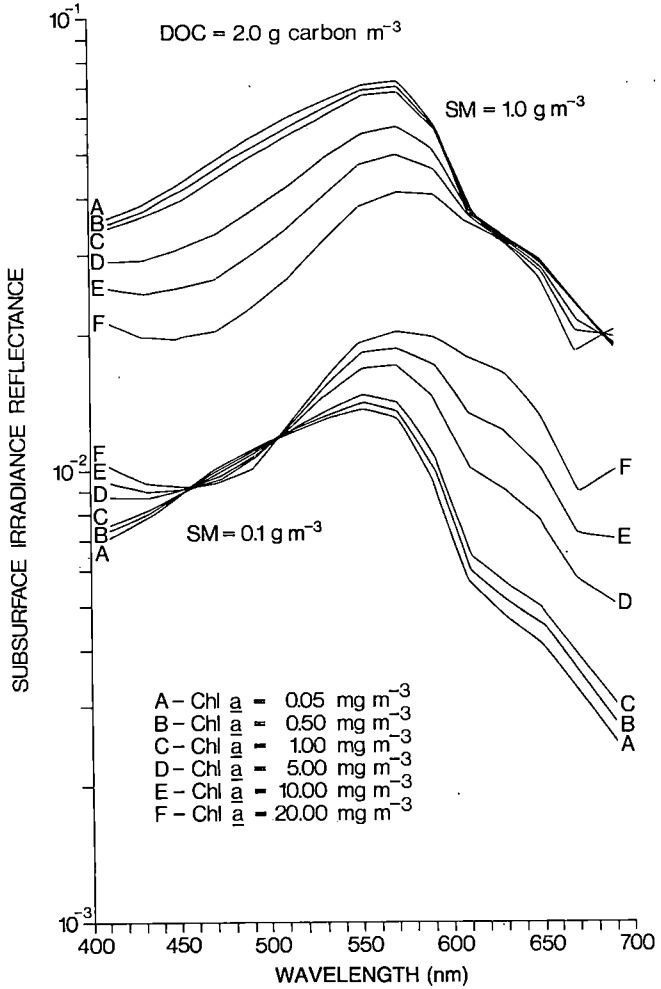

Figure 21. Subsurface irradiance reflectance spectra for various chlorophyll *a* and SM concentrations in a water mass for which the DOC concentration is kept fixed at 2.0 g carbon m^{-3}.

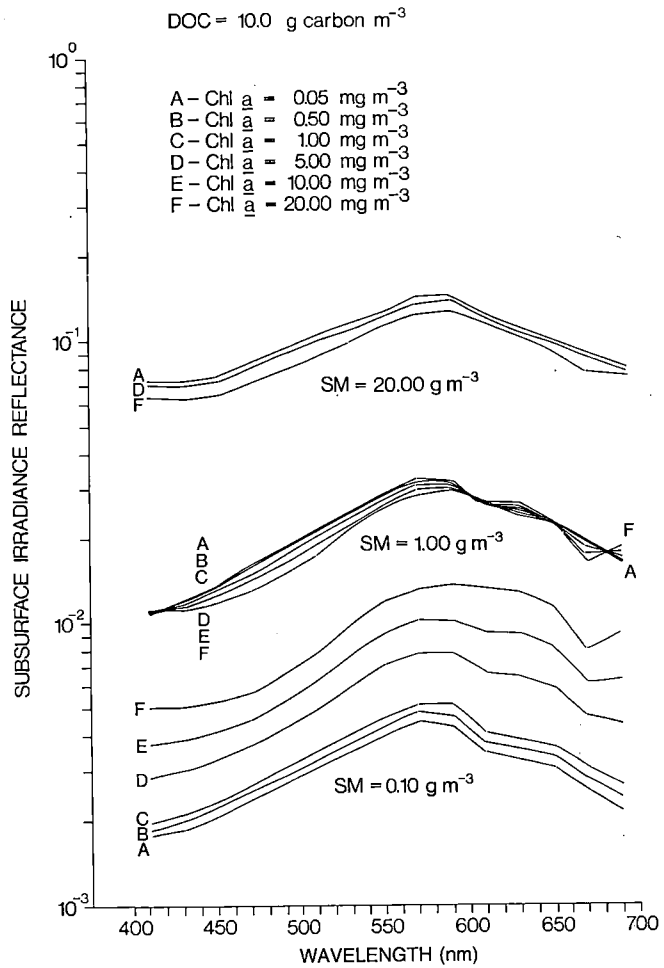

Figure 22. Subsurface irradiance reflectance spectra for various chlorophyll *a* and SM concentrations in a water mass for which the DOC concentration is kept fixed at 10.0 g carbon m^{-3}.

SUBSURFACE IRRADIANCE REFLECTANCE AT A SINGLE WAVELENGTH

To this point, this report has considered subsurface irradiance reflectance spectra (410 to 690 nm), and thus assumes an operational capability of determining such an *in situ* spectrum. Much optical research, however, is conducted with single-band subsurface irradiance meters. This section evaluates the possible application of such single-band devices in estimating the water quality parameters from a single measurement of volume reflectance at one wavelength. Since the visible spectrum may be conveniently divided into blue, green and red components, a single wavelength from each of the blue (450 nm), green (570 nm) and red (650 nm) will be utilized as the basis for ensuing discussions.

From the absorption cross section versus wavelength curves of Figure 2, it is evident that the influence of dissolved organic carbon on subsurface irradiance reflectance is the most pronounced in the blue region of the visible spectrum and the least pronounced in the red region. Consequently, a natural water mass may be approximated, to some extent, by a three-component model (namely pure water, chlorophyll, and suspended minerals) at red wavelengths. Therefore, it could be anticipated that estimations of chlorophyll and/or suspended mineral concentrations from a single wavelength measurement of subsurface irradiance reflectance, if possible at all, might display the highest probability of success if the single wavelength selected were in the red portion of the spectrum. That such an anticipation is, in fact, realized, will emerge from the following discussion.

Figure 23 illustrates the family of relationships that exist between the subsurface irradiance reflectance at 450 nm (blue) and the chlorophyll concentration for a water mass in which the DOC concentration is kept fixed at 2.0 g carbon m^{-3} (a not unreasonable average value for many natural water bodies) and the suspended mineral concentration is permitted to vary between 0 and 20 g m^{-3}. Clearly, the subsurface irradiance relectance at 450 nm (blue) is highly insensitive to change of chlorophyll. Similar relationships between the subsurface irradiance reflectance in the blue and chlorophyll concentrations emerge from a consideration of other DOC concentrations, emphasizing the futility of attempting to estimate chlorophyll concentrations from a single subsurface irradiance reflectance at 450 nm.

In a similar manner, Figure 24 illustrates the situations that arise when the subsurface irradiance reflectance at 570 nm (green) is utilized in an attempt to estimate chlorophyll concentration from a single wavelength measurement. Even though the subsurface irradiance reflectance in the green displays a reasonable sensitivity for a water mass which contains no suspended mineral component, this sensitivity rapidly evaporates once even a trace (< 0.10 g m^{-3}) of suspended mineral is present in the aquatic system.

Figure 25 (similar to Figs. 23 and 24) likewise eliminates a single subsurface irradiance measurement at 650 nm (red) as a means of estimating chlorophyll concentrations, although the sensitivity of the subsurface irradiance reflectance for very clear (in terms of suspended mineral concentrations) water masses is slightly higher for the red than for the green wavelength. Therefore from Figures 23 to 25 it is evident that reliable estimates of chlorophyll concentrations cannot result from single wavelength measurements of the subsurface irradiance reflectance (volume reflectance).

Figure 26 illustrates the family of relationships that exist between the subsurface irradiance reflectance at 450 nm (blue) and the suspended mineral concentration for a water mass in which the DOC concentration is kept fixed at 2.0 g carbon m^{-3} and the chlorophyll concentration is permitted to vary from 0.05 to 20.0 mg m^{-3}. A somewhat promising sensitivity of subsurface irradiance reflectance at the blue wavelength to changes in suspended mineral concentration (coupled with the relative insensitivity of this subsurface irradiance reflectance to changes in chlorophyll concentration as indicated in Fig. 24) appears to be suggested by Figure 26. As indicated earlier, however, the maximum impact of DOC manifests in the blue region of the spectrum. This impact is illustrated in Figure 27 wherein the observable range of subsurface irradiance reflectance values at 450 nm (blue) is plotted as a function of suspended mineral concentration for a water body, which may display a range of DOC concentrations between 0 and 5 g carbon m^{-3} and a range of chlorophyll *a* concentrations between 0.05 and 20.0 mg m^{-3}. The sensitivity of the volume reflectance in the blue to changes in suspended mineral concentration quickly loses its initial attractiveness.

The sensitivity of the subsurface irradiance reflectance at 570 nm (green) to changes in suspended mineral concentration for a water mass containing a fixed DOC concentration of 2.0 g carbon m^{-3} is shown in Figure 28 for several values of chlorophyll concentration. The impact of the presence of chlorophyll on the measured subsurface irradiance reflectance at green wavelengths for small suspended mineral concentrations is clearly more pronounced than the corresponding impact of the presence of chlorophyll on the measured subsurface irradiance reflectance at blue wavelengths. However, the volume reflectance at green wavelengths is less sensitive to changes in DOC concentrations than is the volume reflectance at blue wavelengths. Figure 29 (similar to Fig.27) illustrates the observable range

of subsurface irradiance reflectance values at 570 nm (green) plotted as a function of suspended mineral concentration for a water body which may display a range of DOC concentrations between 0 and 5 g carbon m^{-3} and a range of chlorophyll concentrations between 0.05 and 20.0 mg m^{-3}. While the response of the subsurface irradiance reflectance at 570 nm (green) to changes in suspended mineral concentration will not satisfactorily permit a reliable estimation of suspended mineral concentration from a volume reflectance measurement at a single wavelength in the green region of the spectrum, Figure 29 (for green volume reflectance), nonetheless, displays an obvious improvement in sensitivity over Figure 27 for blue volume reflectance.

The sensitivity of the subsurface irradiance reflectance at 650 nm (red) to changes in suspended mineral concentration for a water mass containing a fixed DOC concentration of 2.0 g carbon m^{-3} is shown in Figure 30 for several values of chlorophyll concentration. The large impact of the presence of chlorophyll on the volume reflectance at red wavelengths observed in water masses containing small concentrations of suspended minerals is an obvious feature of Figure 30. However, when the minimal impact of DOC concentrations on the volume reflectance observable in the red region of the spectrum is also considered, the sensitivity curve of Figure 31 may be constructed. Comparable to Figures 27 and 29, Figure 31 illustrates the observable ranges of subsurface irradiance reflectance values at 650 nm (red) plotted as a function of suspended mineral concentration for a water body which may display a range of DOC concentrations between 0 and 5 g carbon m^{-3} and a range of chlorophyll concentrations between 0.05 and 20.0 mg m^{-3}. Clearly, a reasonable sensitivity to suspended mineral concentration may be ascribed to the subsurface irradiance reflectance at 650 nm (red), particularly for suspended mineral concentrations of more than ~ 0.10 g m^{-3}, and consequently, a single volume reflectance measurement at red wavelengths does appear to possess some capability of estimating suspended mineral concentrations in most natural lake waters.

The asymptotic nature of Figure 31 is also quite apparent. As seen from Equation 7, R(0,650) asymptotically approaches the approximate value $\frac{1}{3} \cdot \frac{Bb(650)}{a(650) + Bb(650)}$ which would render determinations of suspended mineral concentrations of more than ~ 40 g m^{-3} very hazardous. However, in the general range 0.10 g $m^{-3} < C_{SM} < 40$ g m^{-3}, a single volume reflectance measurement at 650 nm may provide a reasonable estimate of suspended mineral concentration despite the competing optical activity resulting from the simultaneous presence of chlorophyll and dissolved organic material within the water mass.

The sensitivity of the subsurface irradiance reflectance at 650 nm is further improved if such single wavelength *in situ* optical measurements are performed within natural waters that do not display an excessive amount of biological activity (such as oceans, oligotrophic and mesotrophic lakes and rivers). Figure 32 illustrates the observable ranges of subsurface irradiance reflectance values at 650 nm plotted as a function of suspended mineral concentration for a water body in which the chlorophyll concentration range is restricted to $0.05 \leq C_{Chl} \leq 5.0$ mg m^{-3}. The increased sensitivity becomes readily apparent.

In summary, therefore, the optical complexities of inland water bodies present overwhelming obstacles to the use of single wavelength measurements of subsurface irradiance reflectance (volume reflectance) as a means of providing water quality indicators. It is totally infeasible to attempt a reliable estimate of the chlorophyll concentration from such single wavelength *in situ* measurements, irrespective of what wavelength is considered. Similarly, the blue and green regions of the visible spectrum are inappropriate wavelength bands with which to attempt an estimation of suspended mineral concentrations (due, in large part, to the interference from dissolved organic material). Despite severe restrictions resulting from the optical interference of chlorophyll concentrations (particularly at low suspended mineral concentrations), however, single wavelength subsurface irradiance measurements in the red region of the visible spectrum do possess some applicability to the estimation of small to moderate concentrations of suspended minerals.

Therefore, if direct measurements of subsurface irradiance reflectance, do, in fact, possess an application to the determination of water quality indicators, it is evident that the entire subsurface irradiance reflectance spectrum must be considered.

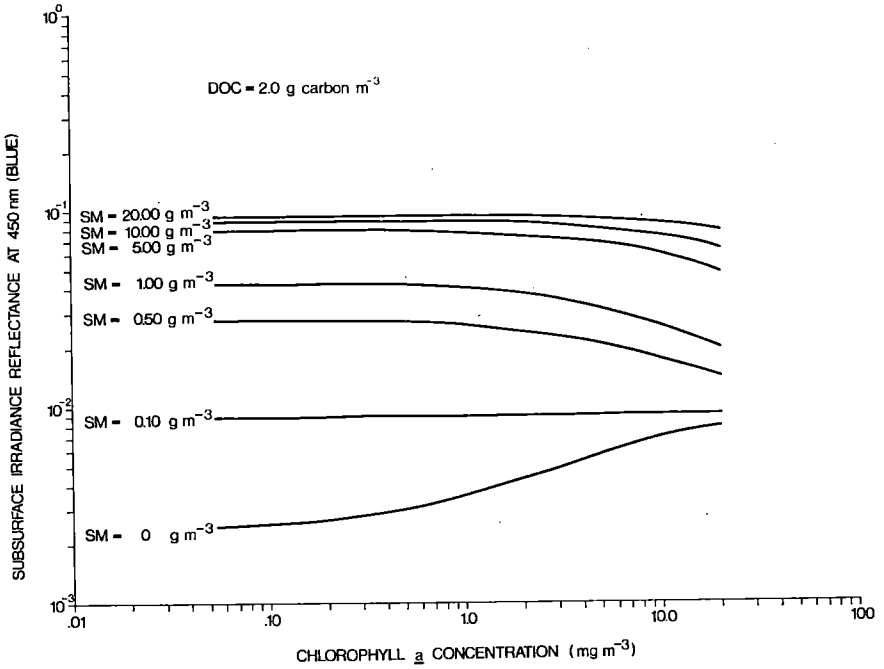

Figure 23. **Relationship between subsurface irradiance reflectance at 450 nm (blue) and chlorophyll *a* concentration for a water mass in which the DOC concentration is kept fixed at 2.0 g carbon m^{-3} and the SM concentration is permitted to vary between zero and 20 g m^{-3}.**

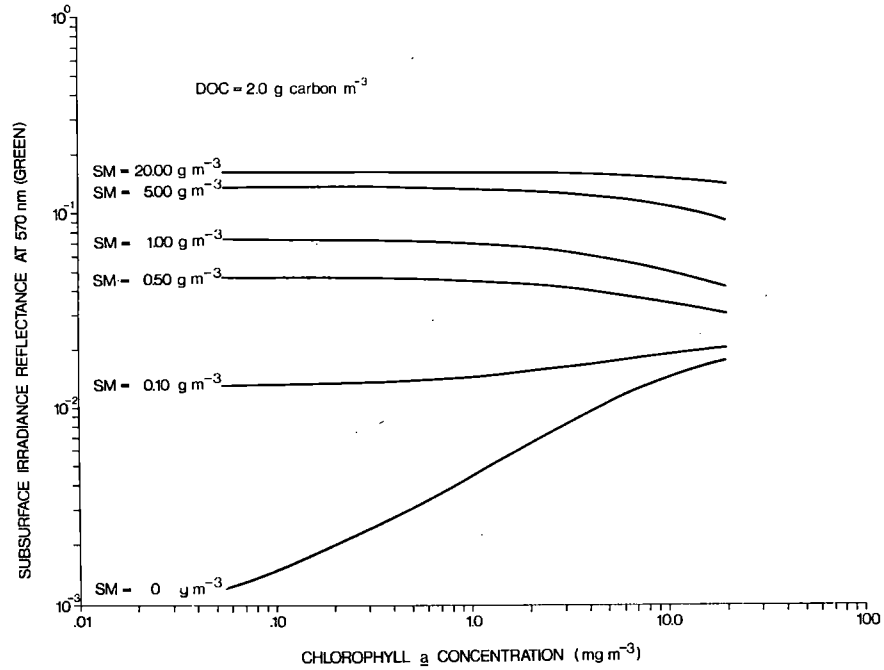

Figure 24. **Relationship between subsurface irradiance reflectance at 570 nm (green) and chlorophyll *a* concentration for a water mass in which the DOC concentration is kept fixed at 2.0 g carbon m^{-3} and the SM concentration is permitted to vary between zero and 20 g m^{-3}.**

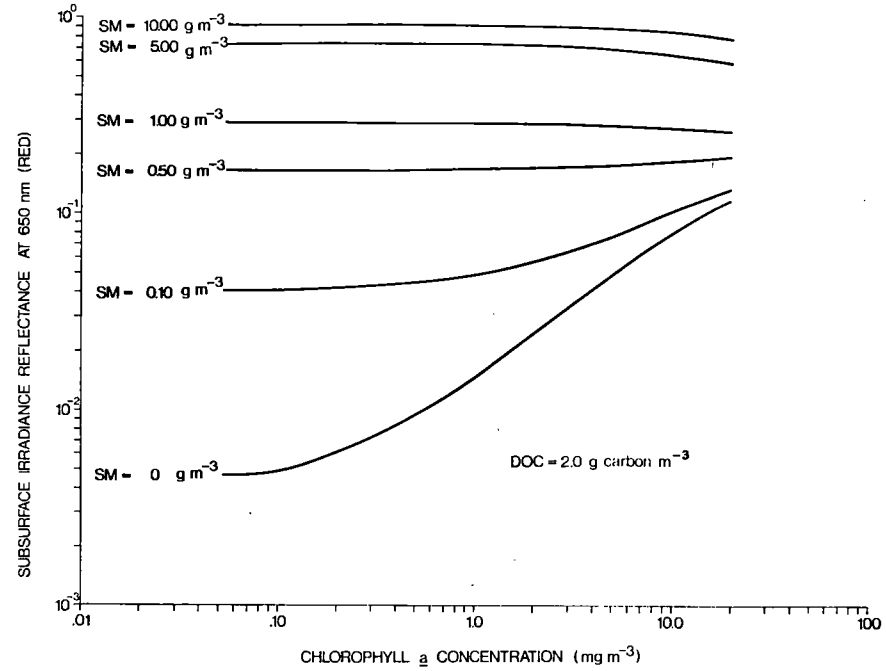

Figure 25. **Relationship between subsurface irradiance reflectance at 650 nm (red) and chlorophyll *a* concentration for a water mass in which the DOC concentration is kept fixed at 2.0 g carbon m^{-3} and the SM concentration is permitted to vary between zero and 10 g m^{-3}.**

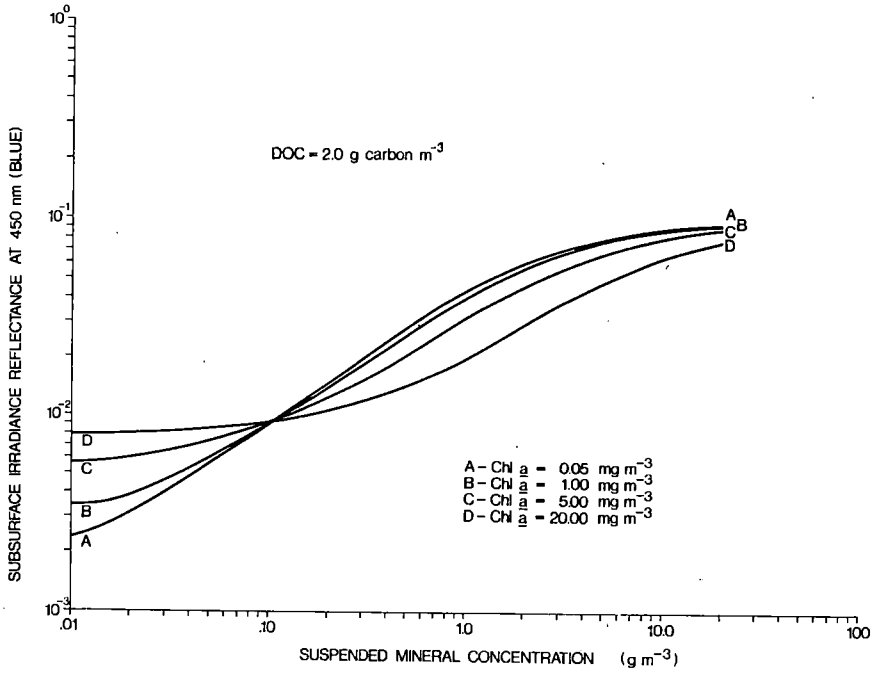

Figure 26. **Relationship between subsurface irradiance reflectance at 450 nm (blue) and SM concentration for several discrete values of chlorophyll *a* concentration in a water mass for which the DOC concentration is kept fixed at 2.0 g carbon m^{-3}.**

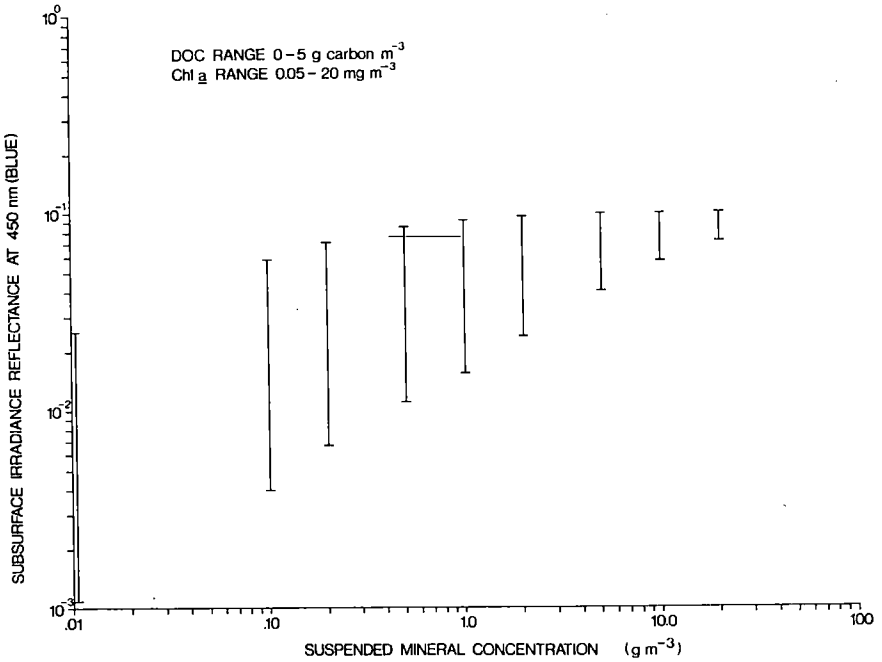

Figure 27. **Relationship between subsurface irradiance reflectance at 450 nm (blue) and SM concentration for a water mass in which the DOC concentration is permitted to vary between zero and 5 g carbon m^{-3} and the chlorophyll *a* concentration, to vary between 0.05 and 20.0 mg m^{-3}.**

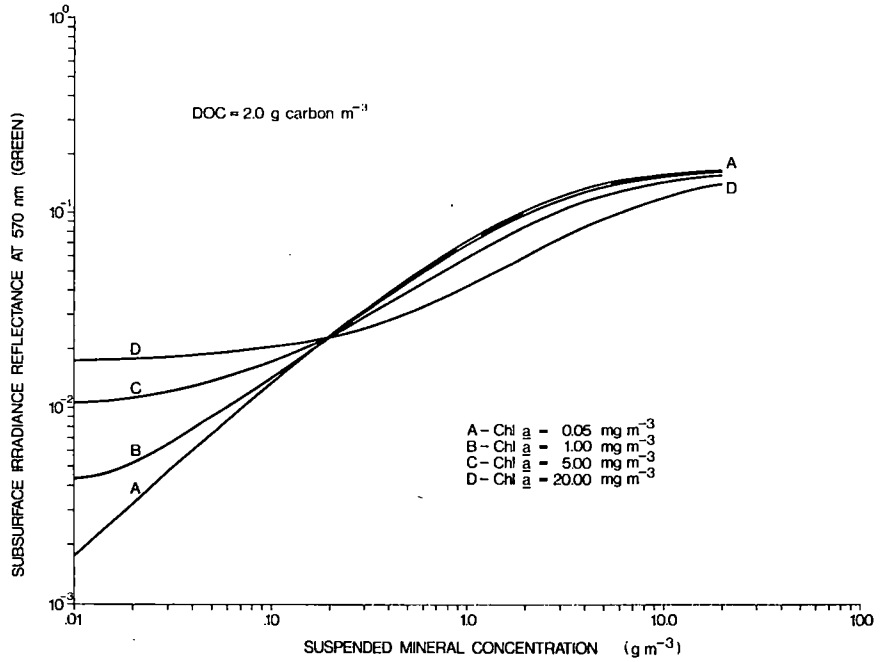

Figure 28. **Relationship between subsurface irradiance reflectance at 570 nm (green) and SM concentration for several discrete values of chlorophyll *a* concentration in a water mass for which the DOC concentration is kept fixed at 2.0 g carbon m^{-3}.**

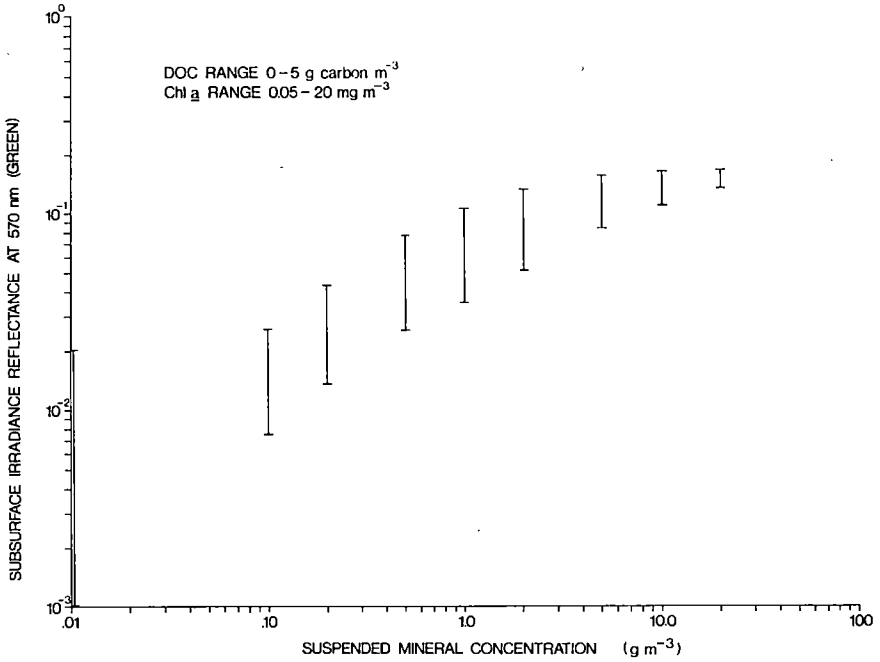

Figure 29. **Relationship between subsurface irradiance reflectance at 570 nm (green) and SM concentration for a water mass in which the DOC concentration is permitted to vary between zero and 5 g carbon m^{-3} and the chlorophyll *a* concentration, to vary between 0.05 and 20.0 mg m^{-3}.**

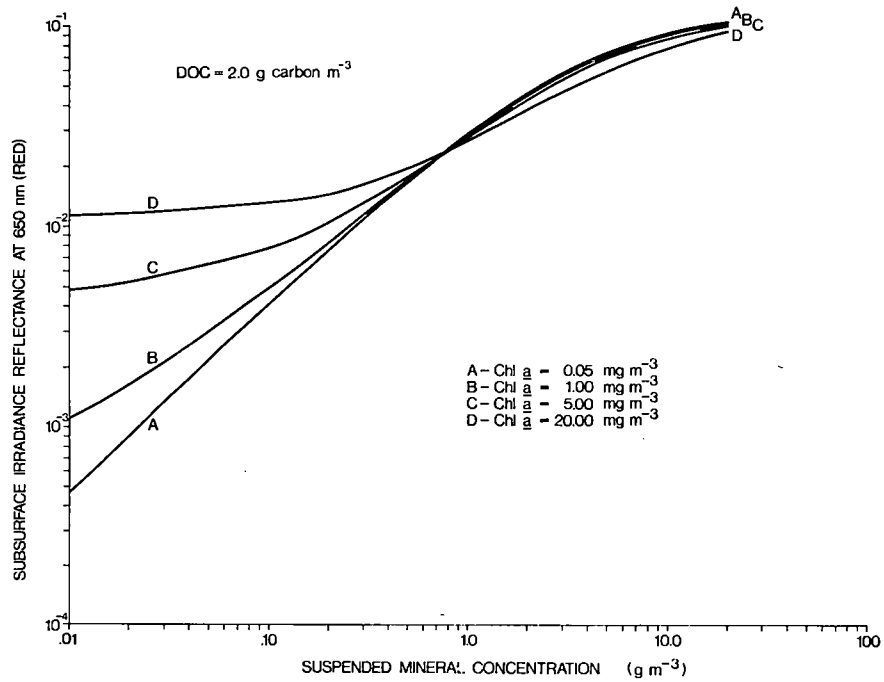

Figure 30. **Relationship between subsurface irradiance reflectance at 650 nm (red) and SM concentration for several discrete values of chlorophyll *a* concentration in a water mass for which the DOC concentration is kept fixed at 2.0 g carbon m^{-3}.**

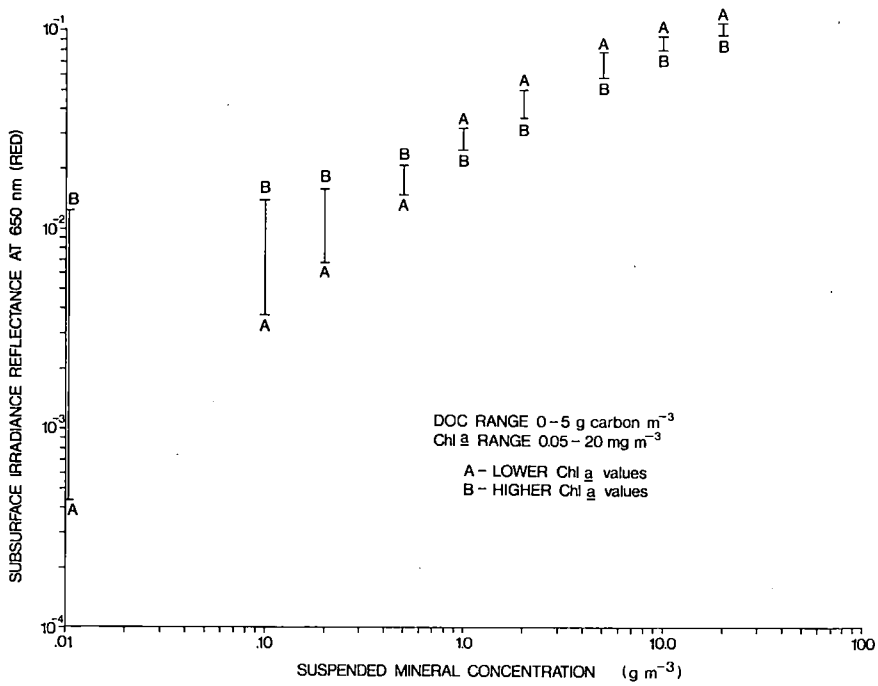

Figure 31. **Relationship between subsurface irradiance reflectance at 650 nm (red) and SM concentration for a water mass in which the DOC concentration is permitted to vary between zero and 5 g carbon m^{-3} and the chlorophyll *a* concentration, to vary between 0.05 and 20.0 mg m^{-3}.**

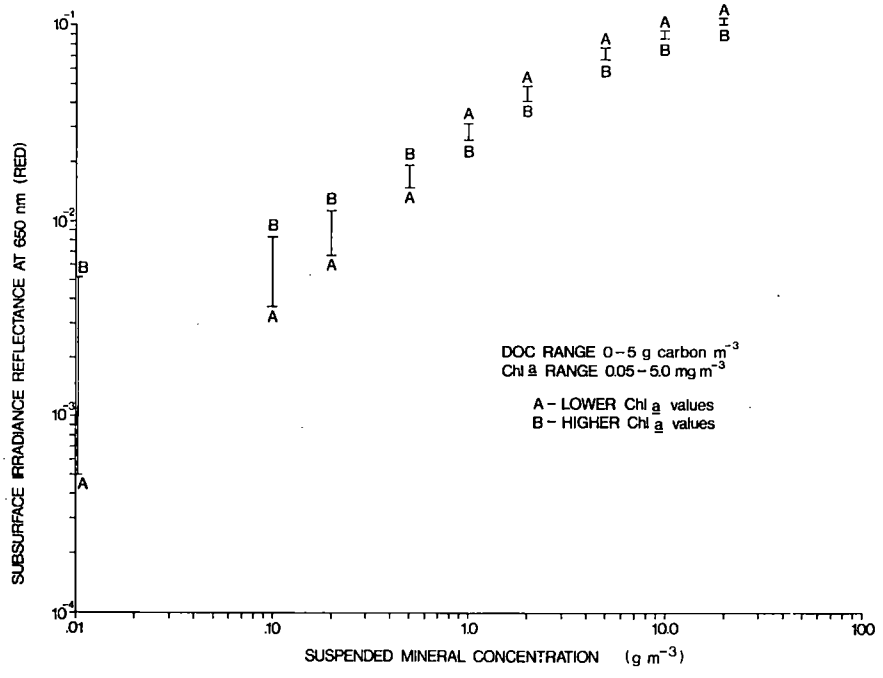

Figure 32. **Relationship between subsurface irradiance reflectance at 650 nm (red) and SM concentration for a water mass in which the DOC concentration is permitted to vary between zero and 5 g carbon m^{-3} and the chlorophyll *a* concentration, to vary between 0.05 and 5.0 mg m^{-3}.**

RELATIONSHIPS AMONG OPTICAL AND WATER QUALITY PARAMETERS

This section will attempt to define, in mathematical terms, the interrelationships between the volume reflectance and the water quality parameters. That is, it investigates the effect on observed volume reflectance spectra of varying chlorophyll, suspended mineral, and dissolved organic carbon concentrations simultaneously. The resulting equations will illustrate the difficulties encountered in attempting a mathematical determination of the water quality parameters from direct measurements of the volume reflectance (subsurface irradiance reflectance) spectrum, indicating the need for a multivariate optimization technique for the extraction of water quality information from such optical spectra. Consequently, the reader may choose to disregard the discussions presented in this section and proceed directly to the next section with no loss of continuity.

Consider a homogeneous water mass made up of concentrations of water, chlorophyll, suspended minerals, and dissolved organic carbon given by C_w, C_{Chl}, C_{SM} and C_{DOC}, respectively. The volume reflectance at wavelength λ, $R(\lambda)$ will be a function of these concentrations and the optical cross sections, that is:

$$R(\lambda) = f(C_w a_w,\ C_{Chl} a_{Chl},\ C_{SM} a_{SM},\ C_{DOC} a_{DOC},\ C_w (Bb)_w,\ C_{Chl} (Bb)_{Chl},\ C_{SM} (Bb)_{SM}) \quad (8)$$

where the wavelength dependence of the optical cross sections has been dropped for simplicity of notation.

The rate of change of volume reflectance with wavelength (i.e., the slope of the measured volume reflectance spectrum at wavelength λ), $\frac{dR(\lambda)}{d\lambda}$, is therefore defined as:

$$\frac{dR(\lambda)}{d\lambda} = \frac{\partial R}{\partial a_w} \cdot \frac{\partial a_w}{\partial \lambda} + C_{Chl} \frac{\partial R}{\partial a_{Chl}} \cdot \frac{\partial a_{Chl}}{\partial \lambda} + C_{SM} \frac{\partial R}{\partial a_{SM}} \cdot \frac{\partial a_{SM}}{\partial \lambda} + C_{DOC} \frac{\partial R}{\partial a_{DOC}} \cdot \frac{\partial a_{DOC}}{\partial \lambda} + \frac{\partial R}{\partial (Bb)_w} \cdot \frac{\partial (Bb)_w}{\partial \lambda} + C_{Chl} \frac{\partial R}{\partial (Bb)_{Chl}} \cdot \frac{\partial (Bb)_{Chl}}{\partial \lambda} + C_{SM} \frac{\partial R}{\partial (Bb)_{SM}} \cdot \frac{\partial (Bb)_{SM}}{\partial \lambda} \quad (9)$$

where C_w has been set to 1, and the partial derivatives of the optical cross sections (which are a function of λ) are defined by the shapes of the curves illustrated in Figures 2 and 3 (with the exception of Figure 3, in which each point would be multiplied by its appropriate $B(\lambda)$).

From Equation 7, the volume reflectance $R(\lambda)$ is given by:

$$R(\lambda) = \sum_{n=0}^{3} r_n \left[\frac{(Bb)(\lambda)}{a(\lambda) + (Bb)(\lambda)}\right]^n = \sum_{n=0}^{3} r_n \left[\frac{u(\lambda)}{v(\lambda)}\right]^n \quad (10)$$

where $u(\lambda) = (Bb)_w + C_{Chl}(Bb)_{Chl} + C_{SM}(Bb)_{SM}$

$$v(\lambda) = a_w + C_{Chl} a_{Chl} + C_{SM} a_{SM} + C_{DOC} a_{DOC} + (Bb)_w + C_{Chl}(Bb)_{Chl} + C_{SM}(Bb)_{SM}$$

Partially differentiating Equation 10 with respect to each of the optical cross sections yields:

$$\frac{\partial R}{\partial a_w} = -\frac{Nu}{v^2}$$

$$\frac{\partial R}{\partial a_{Chl}} = -\frac{N C_{Chl} u}{v^2}$$

$$\frac{\partial R}{\partial a_{SM}} = -\frac{N C_{SM} u}{v^2}$$

$$\frac{\partial R}{\partial a_{DOC}} = -\frac{N C_{DOC} u}{v^2} \quad (11)$$

$$\frac{\partial R}{\partial (Bb)_w} = \frac{N(v-u)}{v^2}$$

$$\frac{\partial R}{\partial (Bb)_{Chl}} = \frac{N C_{Chl} (v-u)}{v^2}$$

$$\frac{\partial R}{\partial (Bb)_{SM}} = \frac{N C_{SM} (v-u)}{v^2}$$

where $N = r_1 + 2r_2 \frac{u}{v} + 3r_3 \frac{u^2}{v^2}$

and r_1, r_2 and r_3 are the coefficients of expansion from Equation 7.

Substituting Equation set 11 into Equation 9 yields:

$$\frac{dR(\lambda)}{d\lambda} = -\frac{Nu}{v^2}\left[\frac{\partial a_W}{\partial\lambda} + C_{Chl}{}^2\,\frac{\partial a_{Chl}}{\partial\lambda}\right.$$

$$\left. + C_{SM}{}^2\,\frac{\partial a_{SM}}{\partial\lambda} + C_{DOC}{}^2\,\frac{\partial a_{DOC}}{\partial\lambda}\right]$$

$$+\frac{N(v-u)}{v^2}\left[\frac{\partial (Bb)_W}{\partial\lambda} + C_{Chl}{}^2\,\frac{\partial (Bb)_{Chl}}{\partial\lambda}\right.$$

$$\left. + C_{SM}{}^2\,\frac{\partial (Bb)_{SM}}{\partial\lambda}\right] \qquad (12)$$

where u, v and N are functions of C_{Chl}, C_{SM} and C_{DOC}, as defined above.

Equation 12 then relates the slope of a directly measured subsurface irradiance reflectance spectrum at wavelength λ to the concentrations of chlorophyll, suspended minerals, and dissolved organic carbon generating that observed spectrum. Obvious difficulties exist in attempting to apply Equation 12 (say, at three discrete values of λ) to estimate, from three simultaneous equations, the values of C_{Chl}, C_{SM} and C_{DOC} describing the water mass. From the nature of the wavelength dependencies of the optical cross sections, it is clear that not only are judicious choices of λ's required but so are very accurate determinations of the slopes. Furthermore, very accurate values of $\frac{dR(\lambda)}{d\lambda}$ are also mandatory, and as is evident, these slope values may be small numerically (in addition to being either positive or negative). Further, the values of N, v and u are themselves functions of C_{Chl}, C_{SM} and C_{DOC} (the parameters being sought). Yet this latter problem may be overcome, at least in principle. Since $u(\lambda) = (Bb)(\lambda)$ and $v(\lambda) = a(\lambda) + (Bb)(\lambda)$, a determination of the bulk inherent properties $(Bb)(\lambda)$ (total backscattering coefficient) and $a(\lambda)$ (total absorption coefficient) in the manner described in the earlier sections of this report can provide the required values of u, v and N.

Clearly, therefore, Equation 12 has, in principle, the capability of providing three equations (at three judiciously selected wavelengths) which may be simultaneously solved for the water quality indicators C_{Chl}, C_{SM} and C_{DOC}. However, the severe onus placed upon precisely determining small values of slopes in both measured and available optical parameter spectra would adversely impact the reliability and reproducibility of such a mathematical calculation. The need to determine $a(\lambda)$ and $(Bb)(\lambda)$ along with each *in situ* measurement of the subsurface irradiance spectrum further renders the use of Equation 12 unattractive. Ideally, a method of extracting the desired water quality indicators from a single measurement of the volume reflectance spectrum should be sought and used. Such a method is described in the next section.

MULTIVARIATE OPTIMIZATION TECHNIQUE

The fundamental problem to be solved is as follows: Given a directly measured subsurface irradiance reflectance spectrum $R(0,\lambda)$, which may be mathematically defined by Equation 7 (i.e. $R(0,\lambda)$ as an expanded function of $a(\lambda)$ and $Bb(\lambda)$, themselves functions of the optical cross sections and the concentrations of chlorophyll, suspended minerals, and DOC), find the values of chlorophyll, suspended minerals, and DOC that generate a subsurface irradiance reflectance spectrum most closely resembling the measured spectrum.

Clearly, a multivariate optimization technique appropriate for estimating "best fit" concentrations of chlorophyll, suspended minerals and dissolved organic carbon should also have application to the solution of an inverse problem, namely: Given directly measured subsurface irradiance spectra and the corresponding concentrations of chlorophyll, suspended minerals and dissolved organic carbon which contribute to the observation of such spectra, find the values of absorption and scattering cross sections (as a function of λ) that generate a subsurface irradiance reflectance most closely resembling the measured spectrum.

This section details the nature of the multivariate optimization technique employed by the Environmental Optics Section of the National Water Research Institute in (a) attempting an extraction of water quality indicators from *in situ* measurements of the subsurface irradiance reflectance spectra in the range 400 to 700 nm and (b) attempting a determination of the optical cross sections from *in situ* measurements of the subsurface irradiance reflectance and water quality measurements performed in concert with the optical measurements.

Some of the mathematical difficulties associated with attempting an analytical solution of Equation 7 have been outlined in the preceding section. However, numerical techniques exist which can circumvent such complexities.

Rewriting Equation 7 in vector form yields:

$$R(0,\underline{a}(\lambda),\underline{Bb}(\lambda),\underline{C}) = \sum_{n=0}^{3} r_n(0)\,[1+(\underline{a}(\lambda)\cdot\underline{C})/(\underline{Bb}(\lambda)\cdot\underline{C})]^{-n} \qquad (13)$$

where

$$\underline{a}(\lambda) = (a_w(\lambda), a_{Chl}(\lambda), a_{SM}(\lambda), a_{DOC}(\lambda))$$

$$\underline{Bb}(\lambda) = (Bb_w(\lambda), Bb_{Chl}(\lambda), Bb_{SM}(\lambda), 0)$$

$$\underline{C} = (1, C_{Chl}, C_{SM}, C_{DOC})$$

Given a measured spectrum $\{S_i\}$ consisting of a set of irradiance reflectances at discrete values of λ (e.g. the 15-point spectrum from 410 to 690 nm in 20-nm increments), the weighted residuals between the measured and theoretical volume reflectances $R(0,\underline{a}_i,\underline{Bb}_i,\underline{C})$ can be written as

$$g_i(\underline{C}) = [S_i - R(0,\underline{a}_i,\underline{Bb}_i,\underline{C})]/R(0,\underline{a}_i,\underline{Bb}_i,\underline{C}) \qquad (14)$$

Here it is assumed that the absorption and backscatter vector functions $\underline{a}$ and $\underline{Bb}$ are known for the homogeneous water mass under consideration, and it is desired to find (at the wavelengths corresponding to $\{S_i\}$) the multidimensional least-squares solution by minimizing over $\underline{C}$ the function

$$f(\underline{C}) = \sum_i g_i^2(\underline{C}) \qquad (15)$$

The value of the concentration vector $\underline{C}$ for which $f(\underline{C})$ is the minimum will then be accepted as defining the parameter concentrations for the water mass that produced the measured subsurface irradiance reflectance spectrum $\{S_i\}$.

The subroutine ZXSSQ (one of the routines available in the International Mathematical and Statistical Library [IMSL, 1980]) is a Levenberg-Marquardt finite difference algorithm appropriate for such multivariate non-linear least-squares optimization applications (Levenberg, 1944; Marquardt, 1963). Given a suitable initial value $\underline{C}_o$, the algorithm will systematically determine a local minimum of $f(\underline{C})$. This value of $f(\underline{C})$ may not, however, be the smallest achievable over the valid range of $\underline{C}$. Consequently, numerous starting points $\{\underline{C}_{oj}\}$ are chosen and the algorithm is permitted to determine the corresponding minima $\{f_j(\underline{C})\}$. The $\underline{C}$ associated with the minimum $f_j(\underline{C})$ of this set is then selected as the appropriate solution. Yet there is no guarantee that any particular starting point $\underline{C}_{oj}$ will result in the algorithm successfully finding any minimum for $f(\underline{C})$, since the algorithm may diverge. Furthermore, a $\underline{C}$ may be found which, although mathematically satisfactory, is physically meaningless (e.g. negative concentrations). To obviate such difficulties, suggestions in the IMSL program notes were implemented in which constraints are placed on $\underline{C}$ such that

$$C_{iMIN} \leq C_i \leq C_{iMAX} \qquad \text{for } i = 2,3,4$$

where the subscript i refers to the ith component of the water mass (e.g. $C_2 = C_{Chl}$, $C_3 = C_{SM}$ and $C_4 = C_{DOC}$), and a transformation from the constrained $\underline{C}$ space to an unconstrained $\underline{W}$ space ($-\infty < W_i < +\infty$) is effected using the error function relationship

$$C_i = C_{iMIN} + (C_{iMAX} - C_{iMIN})(1 + \text{erf}(W_i))/2 \qquad (16)$$

The Levenberg-Marquardt algorithm may also be used in a similar manner to extract the parameter cross sections from a set of volume reflectance and concentration measurements. For this application Equation 7 can be rewritten as:

$$R(0,\underline{C}(\underline{u}),\underline{X}) = \sum_{n=0}^{3} r_n(0)\,[1 + (\underline{C}(\underline{u})\cdot\underline{X})/(\underline{C}'(\underline{u})\cdot\underline{X})]^{-n} \qquad (17)$$

where

$$\underline{X} = (a_w, a_{Chl}, a_{SM}, a_{DOC}, Bb_w, Bb_{Chl}, Bb_{SM}, 0)$$

$$\underline{C}(\underline{u}) = (1, C_{Chl}(\underline{u}), C_{SM}(\underline{u}), C_{DOC}(\underline{u}), 0, 0, 0, 0)$$

$$\underline{C}'(\underline{u}) = (0, 0, 0, 0, 1, C_{Chl}(\underline{u}), C_{SM}(\underline{u}), C_{DOC}(\underline{u}))$$

Here $\underline{u}$ is the vector defining the geographical position of the concentration vector $\underline{C}(\underline{u})$, and $\underline{C}'(\underline{u})$ is merely a rotation of $\underline{C}(\underline{u})$ in the multidimensional space.

Given a set of volume reflectance data $\{S_j\}$ at a wavelength, λ_i, and the corresponding concentration data $\{\underline{C}_j\}$ at a number, j, of stations for which we assume the cross sections are invariant, the weighted residuals, $g_j(\underline{X})$, can be formed:

$$g_j(\underline{X}) = [S_j - R(0,\underline{C}_j,\underline{X})]/R(0,\underline{C}_j,\underline{X}) \qquad (18)$$

and the least-squares solution is again found by minimizing over $\underline{X}$ the function

$$f(\underline{X}) = \sum_j g_j^2(\underline{X}) \qquad (19)$$

As before, appropriate constraints are placed on $\underline{X}$

$$X_{iMIN} \leq X_i \leq X_{iMAX} \qquad \text{for } i = 1,2\ldots7$$

(e.g. $X_1 = a_w$, $X_2 = a_{Chl}$ . . . . . $X_7 = Bb_{SM}$)

and the algorithm is permitted to operate in $\underline{W}$ space according to the error function transformation

$$X_i = X_{iMIN} + (X_{iMAX} - X_{iMIN})(1 + \text{erf}(W_i))/2 \qquad (20)$$

The resulting least-squares solution for $\underline{X}$ is, of course, applicable only to the specific wavelength of the $\{S_j\}$ used,

and the same procedure must be repeated substituting the $\{S_j\}$ corresponding to each wavelength at which $\underline{X}$ is desired. In this way it is possible to determine the entire cross-section spectrum $\underline{X}(\lambda)$.

Although a similar Levenberg-Marquardt procedure is utilized in each instance, the determination of $\underline{X}$ is intrinsically more complex than the determination of $\underline{C}$, since the number of dimensions defining $\underline{X}$ space is double the number of dimensions defining $\underline{C}$ space. A 15-point volume reflectance spectrum from a single station is adequate to enable the extraction of the three variable components of $\underline{C}$ for that station. However, data from considerably more than 15 stations are necessary to extract the seven variable components of $\underline{X}$ and yet successfully avoid divergence of the algorithm. In the absence of a sufficient number of stations, the dimensionality of the $\underline{X}$ extraction must be reduced by supplying fixed cross-section values for some of the $\underline{X}$ components (e.g., the absorption and backscatter cross-section spectra of pure water can be used for a_W and Bb_W).

An additional complication that may arise in the determination of the cross-section spectrum $\underline{X}(\lambda)$ will occur at wavelengths where the absorption and/or backscatter cross section of a component decreases to such an extent that the component's contribution to the volume reflectance becomes comparable in magnitude to the uncertainties in the measured data. The Levenberg-Marquardt algorithm will then be incapable of unambiguously determining the cross section for that component and will instead yield one of the constraint boundaries X_{iMIN} or X_{iMAX}. This also results in the determined cross sections of the other components being unreliable at these wavelengths. Such gaps in the spectrum of $\underline{X}(\lambda)$ may be filled by interpolation or extrapolation utilizing the successfully calculated portions of the $\underline{X}(\lambda)$ spectrum.

Thus, the concentration vector $\underline{C}$ may be efficiently extracted from a given measured volume reflectance spectrum, and in a similar manner the cross-section spectrum $\underline{X}(\lambda)$ may be determined from volume reflectance and concentration data.

APPLICATION OF A WATER QUALITY MODEL TO THE ESTIMATION OF CHLOROPHYLL, SUSPENDED MINERAL, AND DISSOLVED ORGANIC CARBON CONCENTRATIONS IN LAKE ONTARIO

An independent data set of water quality parameters and subsurface irradiance reflectance spectra was obtained in western Lake Ontario, also during the 1979 field season. Using the directly measured optical spectra, the optical cross sections (for the four-component model) depicted in Figures 2 and 3, and the Levenberg-Marquardt multivariate optimization technique discussed in the preceding section, concentrations of suspended minerals, dissolved organic carbon, and chlorophyll *a* (uncorrected for phaeophytin contamination) were predicted and these values compared with the values obtained from laboratory analyses of water samples collected at the same time the optical spectra were measured.

Figure 33 illustrates the comparison between predicted and directly measured suspended mineral concentrations so obtained. The cone of predictability, defined by the dotted lines, represents a predictability to within a factor of two about the line of exact predictability, i.e. a predictability uncertainty of $\pm\log 2$.

Figures 34 and 35 illustrate, in a corresponding manner, the comparison between predicted and directly measured dissolved organic carbon and chlorophyll *a* concentrations, respectively.

It is seen from Figures 33 to 35 that

(a) The four-component water quality model and the optical cross sections of Figures 2 and 3 yield excellent predictive capabilities for suspended mineral concentrations and possibly acceptable predictive capabilities for dissolved organic carbon concentrations.

(b) Predictive capabilities of the four-component water quality model and the optical cross sections of Figures 2 and 3 appear to be virtually nonexistent for chlorophyll *a* concentrations.

Clearly, from Figure 35 (which is characterized by a dramatic underprediction of the chlorophyll *a* concentration) it is seen that near-zero values of chlorophyll *a* concentrations appear not only to satisfy the Levenberg-Marquardt optimization process but also not to interfere with the prediction of reasonable values of both suspended mineral and dissolved organic carbon concentrations. This suggests three salient possibilities: (i) subsurface volume reflectance spectra directly measured in Lake Ontario may be satisfactorily simulated (in general) by varying only concentrations of suspended minerals and dissolved organic carbon; (ii) (which is actually a variation of (i)) the optical cross sections of chlorophyll *a* are less effective in determining the optical properties of inland lakes (particularly for small concentrations of chlorophyll) than are the optical properties of suspended mineral and dissolved organic carbon concentrations; and (iii) the optical cross sections for chlorophyll (taken from Figs. 2 and 3 and

determined for Lake Ontario from the first data set) are inappropriate for the second data set. In reality, all three suggested possibilities are indeed correct, as will be discussed below.

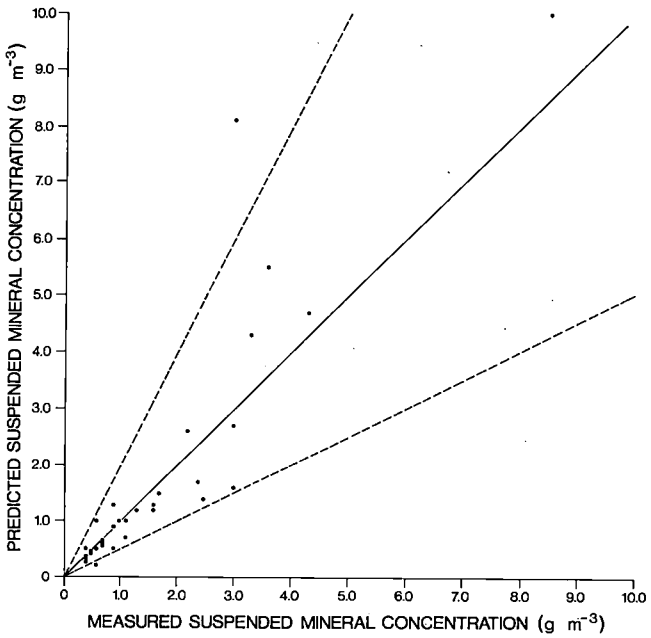

Figure 33. **Comparison between predicted and directly measured SM concentrations (using the cross sections of Figs. 2 and 3).**

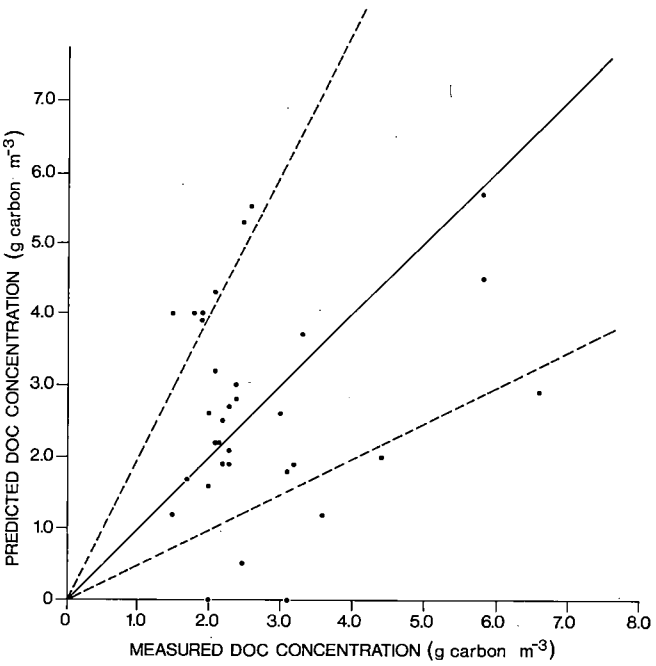

Figure 34. **Comparison between predicted and directly measured DOC concentrations (using the cross sections of Figs. 2 and 3).**

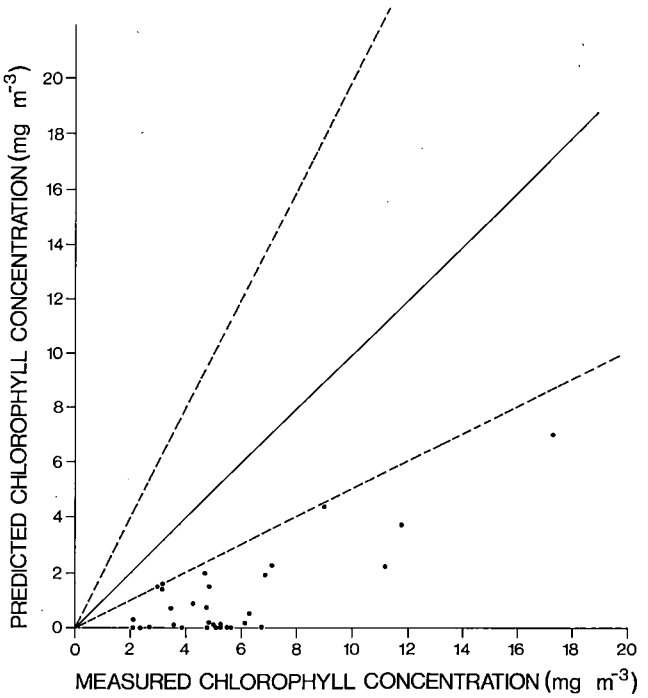

Figure 35. **Comparison between predicted and directly measured chlorophyll *a* concentrations (using the cross sections of Figs. 2 and 3).**

Suggestion (i) is depicted in Figure 36. Therein are shown both the calculated "best fit" subsurface irradiance optical spectrum (joined points) and the experimentally measured subsurface irradiance reflectance spectrum (unjoined points) for a typical relatively nearshore station (within the Niagara plume) in western Lake Ontario. The predicted (calculated) water quality parameters resulting in the "best fit" spectrum are listed, along with the measured values of the water quality parameters at that station, and it is immediately seen that the Levenberg-Marquardt analyses supplied reasonable values of suspended mineral and DOC concentrations while predicting a zero concentration of chlorophyll *a*.

The presence of chlorophyll in the water mass in this instance actually diminishes the ability of the water quality model to simulate the experimentally measured subsurface irradiance reflectance spectrum at this station. This is seen from Figure 37 wherein two calculated optical spectra (for the cross sections of Figs. 2 and 3) are compared with the actually measured optical spectrum. The solid line depicts the predicted optical spectrum for a water mass possessing concentrations of chlorophyll *a*, suspended minerals and dissolved organic carbon close to those actually measured at the station (Chl *a* is taken as 5.0 mg per cubic metre; SM is taken as 5.0 g per cubic metre; DOC is taken as 2.0 g carbon per cubic metre). The dotted line depicts

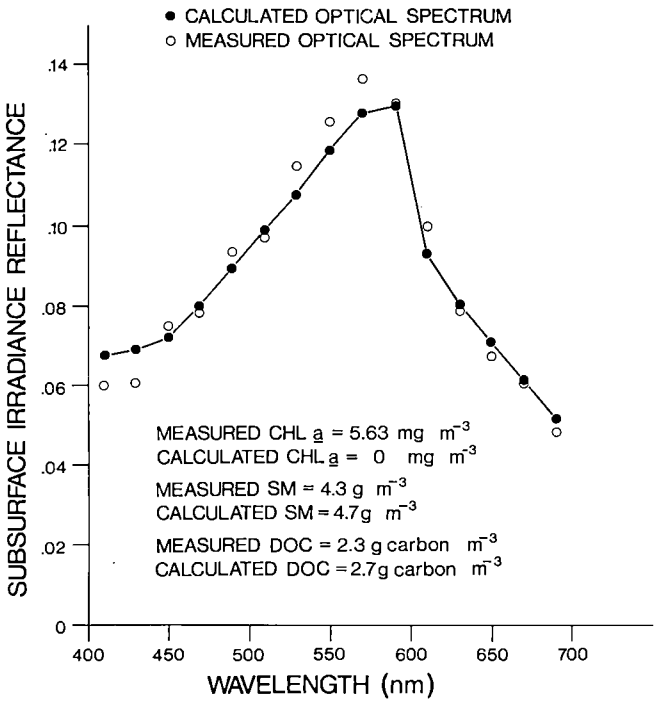

Figure 36. **Comparison between the calculated "best fit" and directly measured subsurface irradiance reflectance spectra for a Niagara plume station in western Lake Ontario (using the cross sections of Figs. 2 and 3).**

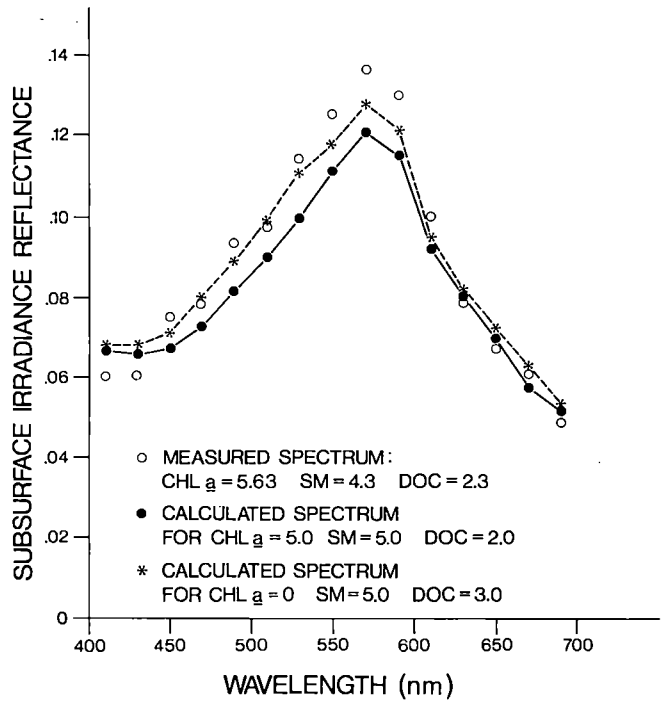

Figure 37. **Comparison between the directly measured subsurface irradiance reflectance spectrum of Figure 36 and two calculated subsurface irradiance reflectance spectra (using the cross sections of Figs. 2 and 3 and two sets of water quality parameters).**

the predicted optical spectrum for a water mass possessing concentrations of chlorophyll *a*, suspended minerals, and dissolved organic carbon close to those predicted by the Levenberg-Marquardt optimization technique (Chl *a* is taken as zero; SM is taken as 5.0 g per cubic metre; DOC is taken as 3.0 g carbon per cubic metre). A distinct improvement in curve fitting is readily realized by the removal of chlorophyll from the aquatic system.

The general shape of the directly measured subsurface irradiance reflectance spectrum (i.e., a distinct peak in the green wavelength region) shown in Figure 36 is almost always observed in Lake Ontario throughout the field season for both nearshore stations and stations substantially offshore. This is illustrated in Figure 38, wherein directly measured volume reflectance spectra are illustrated for both nearshore and midlake stations visited during May, July and September. Although the actual magnitudes of the observed irradiance reflectance (volume reflectance) may vary (a direct consequence of the spatial and temporal variabilities of the water quality parameters at the stations), the pronounced peak at mid-wavelengths is a readily recognizable feature of each optical spectrum. Salient point (ii) may be

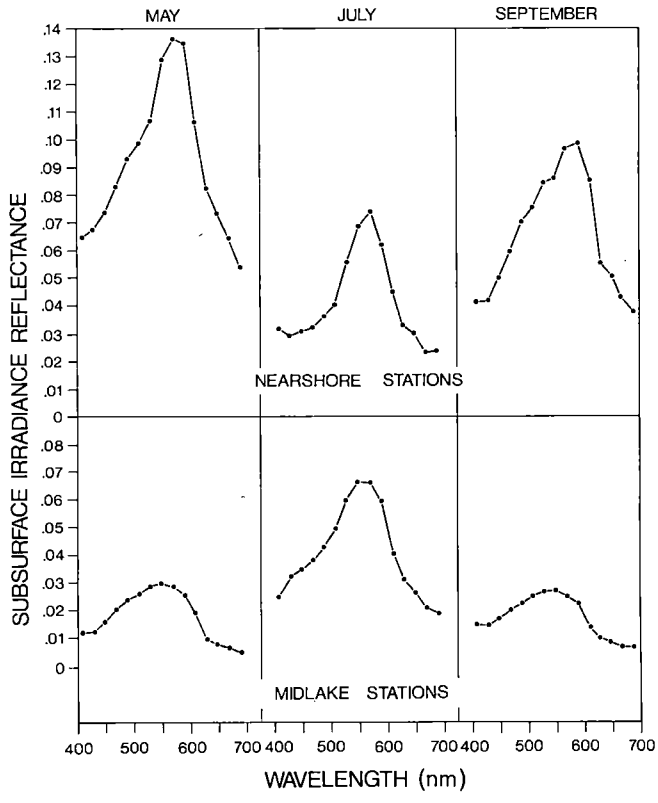

Figure 38. **Representative examples of directly measured subsurface irradiance reflectance spectra obtained at nearshore and midlake stations in Lake Ontario throughout the field season.**

readily seen from a consideration of Figures 37 and 38 and Figures 18 and 19.

As evident from Figures 18 and 19, the addition of either suspended minerals or chlorophyll *a* (to a water mass containing ~2.0 g carbon per cubic metre) will produce a distinct maximum in the mid-wavelength region of the visible spectrum. Furthermore, as seen from Figures 18 and 19 (and discussed earlier in this report), the effect of the relative concentrations of chlorophyll *a* and suspended minerals normally found in inland lakes will be such as to make the suspended mineral concentrations more effective than the chlorophyll concentrations in generating the "green" maximum in the measured volume reflectance spectrum.

Suggestion (iii) was investigated by using the Levenberg-Marquardt optimization method to obtain a new set of optical cross sections for chlorophyll *a* (uncorrected for phaeophytin contamination). Optical and water quality data collected from the western Lake Ontario test sites during May and July 1979 were utilized. The cross sections for suspended minerals and dissolved organic carbon were retained from Figures 2 and 3, and the optimization technique was used to determine new values of a_{Chl} and b_{Chl} throughout the visible spectrum. For the second data set, however, additional information concerning the composition of the above surface-impinging radiation was also available and therefore utilized. Since the coefficients $r_n(0)$ in Equation 7 are functions of the incident radiance distribution (Gordon *et al.*, 1975) (a direct consequence of the fact that volume reflectance is one of the apparent properties of a water mass), the measured volume reflectance will be influenced by both the solar zenith angle (time of day) and the diffuse fraction of the incident downwelling irradiance. This will be true irrespective of changes in the concentrations of the suspended and dissolved constituents of the water mass (see also discussions in Jerome *et al.*, 1982).

Figure 39 (adapted from Table B.3.2 of Moniteq Ltd., 1981) presents the fraction of the above-water downwelling irradiance that is diffuse for each of the months during which the independent data set was obtained. Figure 39 was then used to generate an appropriate set of $r_n(0)$ coefficients corresponding to each fraction, and these coefficients were inserted into Equation 7 prior to the inverse Levenberg-Marquardt analysis.

The resulting Levenberg-Marquardt analysis yielded b_{Chl} values which were essentially in agreement with the b_{Chl} values obtained previously. The a_{Chl} values obtained, however, were significantly different from the a_{Chl} values previously obtained, as illustrated in Figure 40. Although the two data sets agree reasonably well in the high wavelength red portion, the values of a_{Chl} obtained from the second data set (optimization method) for $\lambda < \sim 600$ nm are consistently about a factor of two lower than the values of a_{Chl} obtained from the first data set (multiple regression method).

Utilizing the Levenberg-Marquardt optimized values of a_{Chl} (b_{Chl} and all other cross-section values as shown in Figs. 2 and 3) and the directly measured subsurface irradiance reflectance spectra, the optimization technique (incorporating the incident radiance distribution dependence of $r_n(0)$) was once again used to estimate the water quality indicators that would generate "best fit" simulations to the observed volume reflectance spectra.

Figure 41 (directly comparable to Fig. 36) illustrates the comparison between the directly measured subsurface irradiance reflectance spectrum (unjoined points) and the calculated "best fit" subsurface irradiance reflectance spectrum (joined points) resulting from the use of the modified values of a_{Chl}. It is seen that the Levenberg-Marquardt optimization technique, in addition to predicting acceptable values for suspended mineral and dissolved organic carbon concentrations for the station, also predicts an acceptable value for chlorophyll concentration.

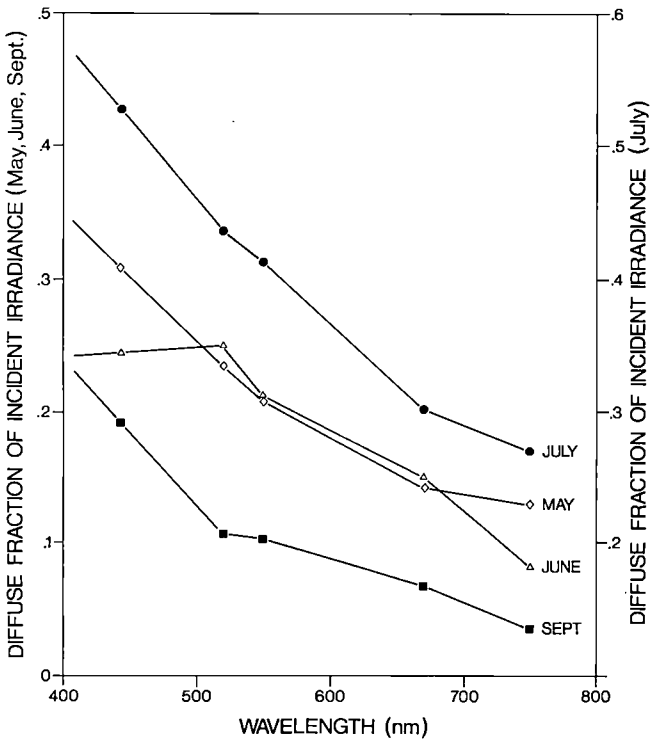

Figure 39. **The wavelength dependence of the diffuse fraction of the above-water downwelling irradiance throughout the field season.**

Figures 42, 43 and 44 illustrate the comparison between the predicted and directly measured concentrations of suspended minerals, dissolved organic carbon, and chlorophyll *a*, respectively. These figures may be directly compared with Figures 33 to 35, the only difference between the two sets of results being that Figures 42 to 44 were generated from the addition of an incident radiance distribution dependence of $r_n(0)$ and the use of the dotted curve (Fig. 40) for the spectral dependence of a_{Chl}.

A consideration of Figures 42 to 44 indicates the following:

(a) The predictive capabilities of the four-component optical model with respect to suspended mineral and dissolved organic carbon concentrations, although impacted to some extent by the use of the modified chlorophyll *a* absorption cross sections, do not appear to be affected to any statistically significant degree.

(b) A very noticeable improvement in the predictive capabilities of the four-component optical model for chlorophyll *a* concentrations, however, is certainly realized by the use of the modified chlorophyll *a* absorption cross sections. Most underpredicted chlorophyll *a* concentrations (Fig. 44) were observed during the month of September. This is more clearly seen from Figure 45, which subdivides the information plotted in Figure 44 into the months (May, July, September) during which the volume reflectance measurements were taken.

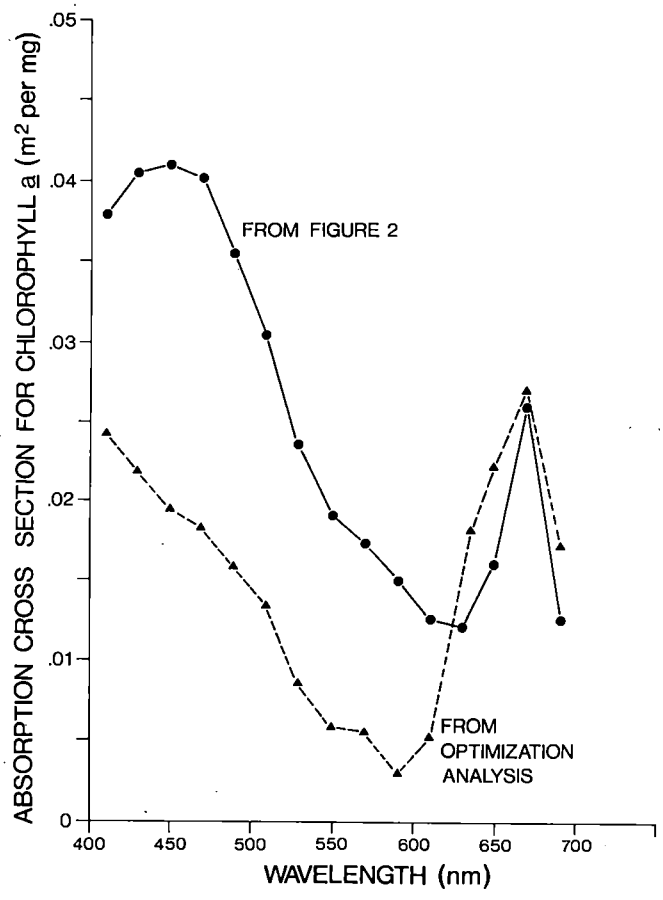

Figure 40. A comparison of the chlorophyll *a* absorption cross sections obtained from two optical/water quality data sets.

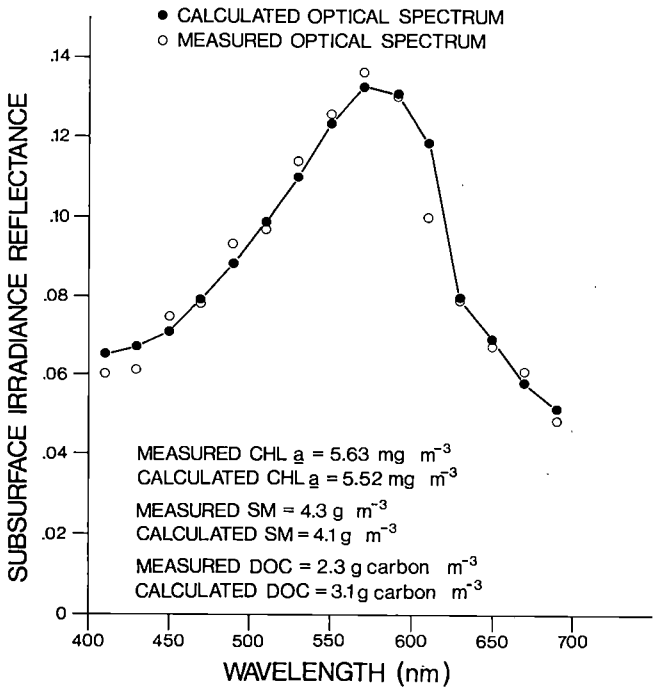

Figure 41. Comparison between the calculated "best fit" and directly measured subsurface irradiance reflectance spectra for the Niagara plume station of Figure 36 (using the modified chlorophyll *a* absorption cross-section values).

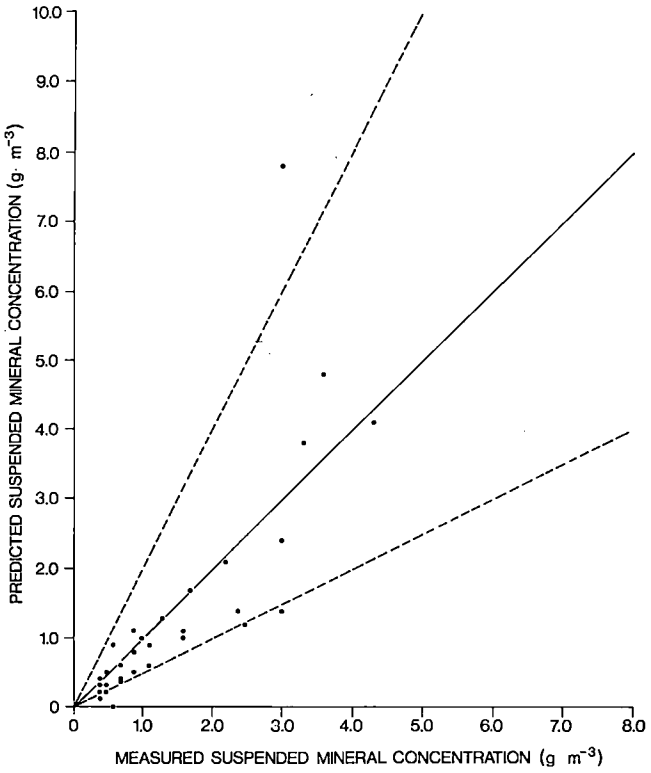

Figure 42. Comparison between predicted and directly measured SM concentrations (using the modified chlorophyll *a* absorption cross sections of Fig. 40).

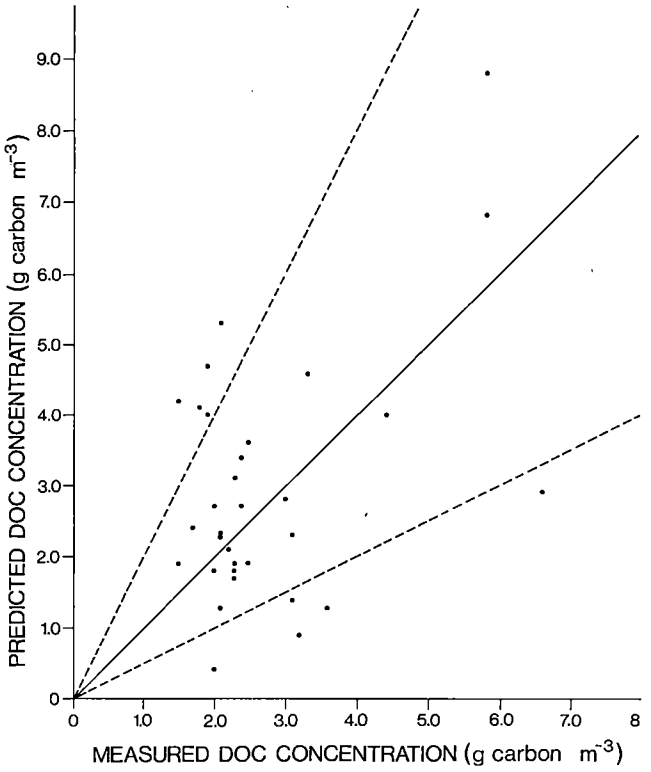

Figure 43. Comparison between predicted and directly measured DOC concentrations (using the modified chlorophyll *a* absorption cross sections of Fig. 40).

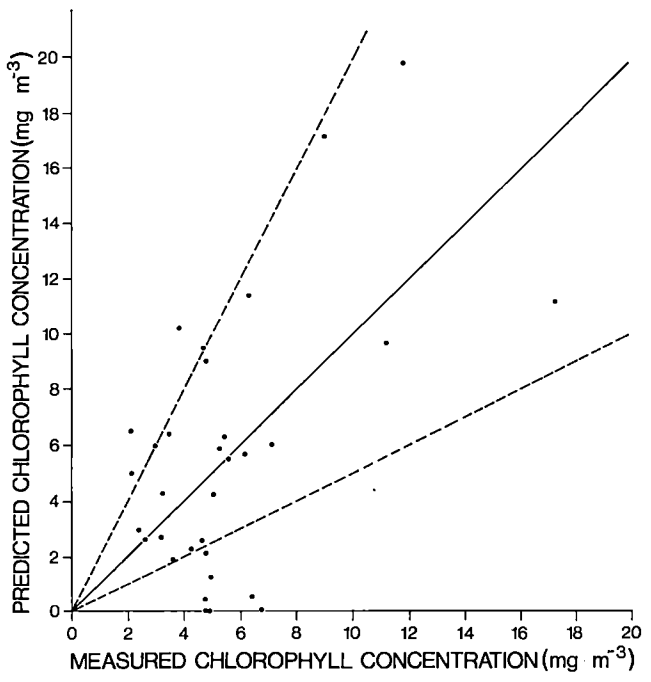

Figure 44. Comparison between predicted and directly measured chlorophyll *a* concentrations (using the modified chlorophyll *a* absorption cross sections of Fig. 40).

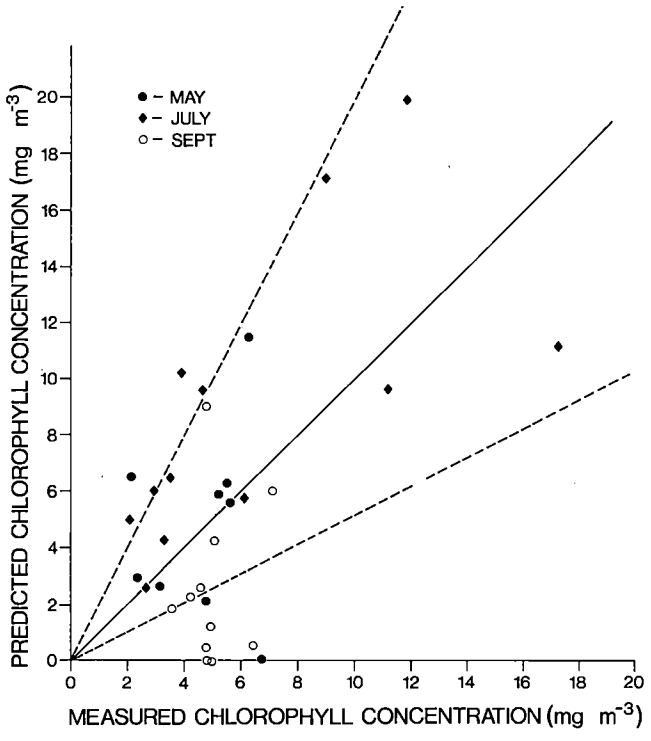

Figure 45. Comparison between predicted and directly measured chlorophyll *a* concentrations (using the modified chlorophyll *a* absorption cross sections of Fig. 40) on a monthly basis.

DIFFICULTIES ASSOCIATED WITH CHLOROPHYLL PREDICTIONS

The physical principles upon which the multi-component optical models described in this report are based, are sound, to within the limitations presented and the current level of aquatic understanding. The absorption and scattering properties of the suspended and dissolved materials comprising inland water masses, along with the properties of the impinging above-surface irradiance, will dictate the subsurface irradiance reflectance (volume reflectance) spectra that will be experimentally measured within those water masses. Water quality indicators (organic and inorganic components of natural water masses) exist as absorption and scattering centres throughout the water column. Thus it logically follows that (within limits of possible ambiguities) simulated volume reflectance spectra generated from known concentrations of water quality indicators could be mathematically compared with measured volume reflectance spectra as a means of estimating the *in situ* concentrations of the water quality indicators that have contributed to the observance of those spectra.

The critical ingredient to such predictive methodology, however, is a precise knowledge of the optical cross sections (absorption and scattering on a per unit concentration basis) of the constituent materials of the water mass in question. While there is an increasing effort, on a world-wide scale, to obtain such precise information, the results of such efforts to date have been far from universally applicable. Certainly, there is general agreement concerning the observed range of such cross-section values and the realization that such cross sections will be not only geographically and subspecies dependent but also temporally dependent. Consequently, a major obstacle to such optical research has been an inherent inability to reproduce experimentally equivalent and/or reliably extrapolatable values for such critical parameters. Our own work in Lake Ontario directly reflects this frustration. Two independent coordinated optical/water quality data sets were obtained in western Lake Ontario during the 1979 field season. Although similar wavelength spectra for the absorption and scattering cross sections of suspended minerals and dissolved organic carbon and for the scattering cross section of chlorophyll appear to be reasonably appropriate for both of the data sets, each of the data sets appears to require significantly dissimilar absorption cross-section spectra for chlorophyll (Fig. 40). Within these cross-section restraints, the four-component optical model possesses a water quality indicator predictability to within a factor of two. The value of such water quality predictability is, of course, a moot point and will not be discussed further here.

This observed uncertainty (i.e., the uncertainty with respect to an appropriate value for a specific species at a specific spatial location and/or temporal location within a biological growth cycle) is currently being observed by many workers. Recently, Morel and Bricaud (1981) have discussed the problems that originate from the inconstancy of the absorption cross section for chlorophyll *a* and have illustrated that large departures from constancy exist not only for several distinct species of chlorophyll-bearing cells but also for variations (cell size, cell structure, cell stability, etc.) within the cells of the same species.

A typical representation of the vast discrepancies that exist among various determinations of a_{Chl} is shown in Figure 46 wherein are plotted not only the apparently conflicting results of the current work but also the results of other workers. Several features are immediately evident from the limited data shown in Figure 46:

(a) There is, in general, reasonable agreement concerning the absorption peak at the red end of the visible spectrum (although our earlier work [Bukata *et al.*, 1981a] along with the work of other investigators concerning the NIMBUS-G satellite bands failed to extract a significant peak at these wavelengths).

(b) Very large departures from constancy are observed at the blue end of the spectrum, as is the existence of a possible absorption peak near 450 nm. Notice that the absorption curve resulting from the first data set in Lake Ontario (curve B) displays a distinct absorption peak in the blue, while the absorption curve resulting from the second data set in Lake Ontario (curve C) does not.

(c) The various curves illustrated in Figure 46 display variable rising and falling slopes. As discussed earlier, such variable slopes may dramatically impact the shape of experimentally measured subsurface irradiance profiles.

(d) The Lake Ontario curve C illustrated in the figure appears to be a lower-limit envelope to the plotted data. This is, in fact, not a valid conclusion, since many other workers (data not shown) have obtained smaller values of a_{Chl} than comprise curve C, just as values of a_{Chl} larger than those comprising curve A′ have likewise been observed.

The difficulties encountered in the prediction of chlorophyll *a* from optical measurements and methodologies may be readily appreciated from a consideration of Figure 46. These difficulties notwithstanding, however, the results of this investigation do appear somewhat encouraging. Lake Ontario displays a high degree of optical complexity, and although Lake Ontario may be representative of optically complex waters, it is not necessarily representative

of most inland water masses. A four-component optical model (even with inherent uncertainties in the per unit absorption and scattering properties of the chlorophyll-bearing components) has been shown to possess the capability of predicting to within a factor of two simultaneous concentrations of chlorophyll, suspended minerals, and dissolved organic carbon in Lake Ontario. It is certainly reasonable to conclude that such predictability might be dramatically improved for optically less complex waters.

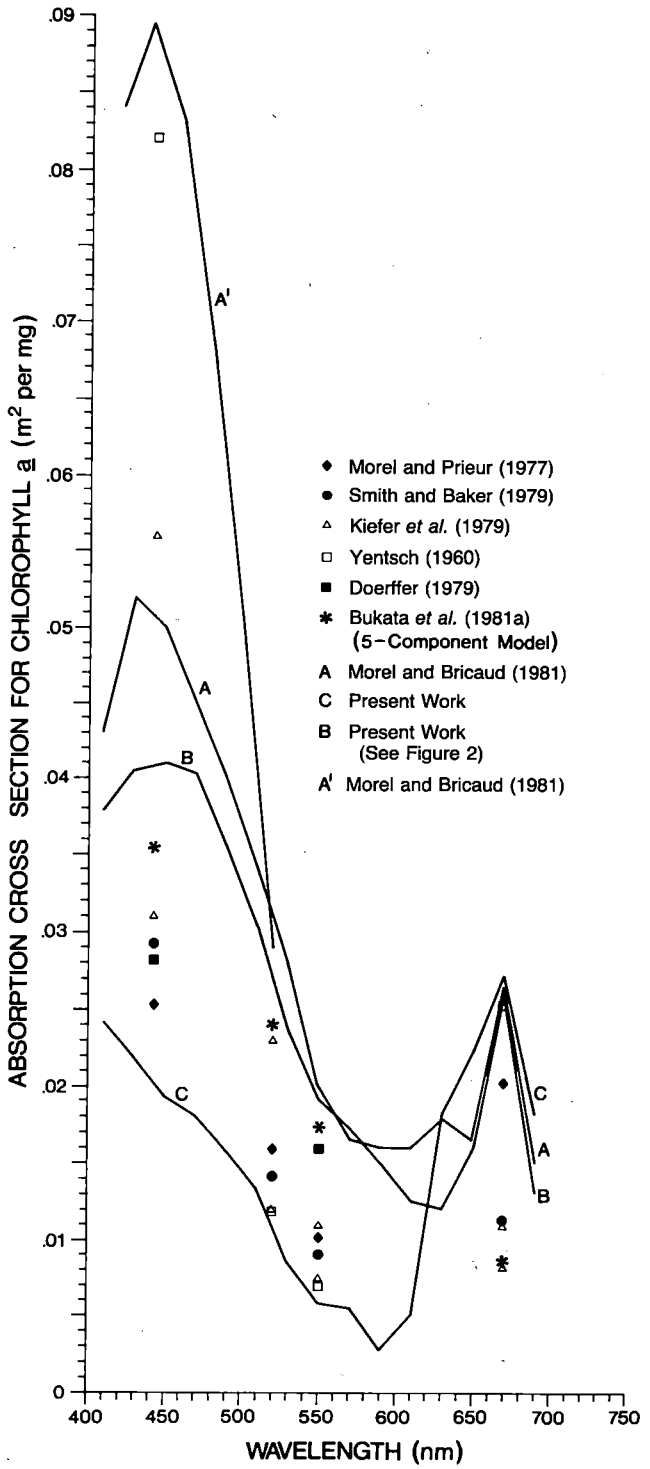

Figure 46. **An intercomparison of a number of independent attempts to determine the absorption cross sections of chlorophyll *a*.**

REFERENCES

Bukata, R.P., J.H. Jerome, J.E. Bruton and S.C. Jain. 1979. Determination of inherent optical properties of Lake Ontario coastal waters. Appl. Opt. 18: 3926-3932.

Bukata, R.P., J.H. Jerome, J.E. Bruton, S.C. Jain and H.H. Zwick. 1981a. Optical water quality model of Lake Ontario. 1. Determination of the optical cross sections of organic and inorganic particulates in Lake Ontario. Appl. Opt. 20: 1696-1703.

Bukata, R.P., J.E. Bruton, J.H. Jerome, S.C. Jain and H.H. Zwick. 1981b. Optical water quality model of Lake Ontario. 2. Determination of chlorophyll *a* and suspended mineral concentrations of natural waters from submersible and low altitude optical sensors. Appl. Opt. 20: 1704-1714.

Bukata, R.P., J.H. Jerome and J.E. Bruton. 1981c. Validation of a five-component optical model for estimating chlorophyll *a* and suspended mineral concentrations in Lake Ontario. Appl. Opt. 20: 3472-3474.

Burns, N.M. 1980. Canada Centre for Inland Waters (private communication).

Di Toro, D.M. 1978. Optics of turbid estuarine waters: approximations and applications. Water Res. 12: 1059–1068.

Doerffer, V.R. 1979. The distribution of substances in the Elfe-Estuary determined by remote sensing. Arch. Hydrobiol. 43: 119-224.

Gordon, H.R., O.B. Brown and M.M. Jacobs. 1975. Computed relationships between the inherent and apparent optical properties of a flat homogeneous ocean. Appl. Opt. 14: 417-427.

Hulburt, E.O. 1945. Optics of distilled and natural water. J. Opt. Soc. Am. 35: 698-705.

IMSL. 1980. The IMSL Library Reference Manual, Edition 8 (revised June 1980), International Mathematical and Statistical Libraries, Inc., Houston.

Jain S.C., H.H. Zwick, W.D. McColl, R.P. Bukata and J.H. Jerome. 1980. Combined Coastal Zone Color Scanner (CZCS), aircraft, and *in situ* water quality remote sensing experiment in Lake Ontario. Proc. Soc. Photo-Op Instrum. Eng. 208: 178-188.

Jerome, J.H., J.E. Bruton and R.P. Bukata. 1982. Influence of scattering phenomena on the solar zenith angle dependence of in-water irradiance levels. Appl. Opt. 21: 642-647.

Kiefer, D.A., R.J. Olson and W.H. Wilson. 1979. Reflectance spectroscopy of marine phytoplankton. Part 1. Optical properties as related to age and growth rate. Limnol. Oceanogr. 24: 664-672.

Levenberg, K. 1944. A method for the solution of certain non-linear problems in least squares. Quant. Appl. Math. 2: 164-168.

Marquardt, D.W. 1963. An algorithm for least-squares estimation of nonlinear parameters. J. SIAM, 11(2).

Moniteq Ltd. 1981. Water quality remote sensing report. Appendices. DSS Contract No. 19SQ.23413-8-1345, Table B.3.2, p. 22.

Morel, A. and A. Bricaud. 1981. Theoretical results concerning light absorption in a discrete medium, and application to specific absorption of phytoplankton. Deep-Sea Res. 11: 1375–1393.

Morel, A. and L. Prieur. 1977. Analysis of variations in ocean color. Limnol. Oceanogr. 22: 709–722.

Smith, R.C. and K.S. Baker. 1979. Optical classification of natural waters. Limnol. Oceanogr. 23: 260–267.

Yentsch, C.S. 1960. The influence of phytoplankton pigments on the color of sea water. Deep-Sea Res. 7: 1–9.

Zwick, H.H., S.C. Jain and R.P. Bukata. 1980. A satellite airborne and *in-situ* water quality experiment in Lake Ontario. Proc. ISPRA Workshop on EURASEP Ocean Color Scanner Exp., pp. 181–198.

APPENDIX

GLOSSARY OF TERMS

Quantity of radiant energy, Q — The quantity of energy transferred by radiation.

Q in joules (J)

Radiant flux, Φ — The rate of flow of radiant energy.

$$\Phi = \frac{Q}{t} \text{ in watts (W)}$$

Radiant intensity, I — The flux radiated from an element of surface per unit solid angle $\partial\omega$.

$$I = \frac{\partial\Phi}{\partial\omega} \text{ in W sr}^{-1}$$

Radiance, L — The radiant flux per unit of solid angle $\partial\omega$ per unit of projected area $\partial A \cos\Theta$, where ∂A is the unit of surface area and Θ is the angle between the incident radiant flux and the normal to the surface area.

$$L = \frac{\partial^2\Phi}{\partial A \cos\Theta \, \partial\omega} \text{ in W m}^{-2} \text{ sr}^{-1}$$

Irradiance, E — The radiant flux per unit of area ∂A.

$$E = \frac{\partial\Phi}{\partial A} \text{ in W m}^{-2}$$

Downwelling irradiance,

$$E_d = \int_{\Phi=0}^{2\pi} \int_{\Theta=0}^{\pi/2} L(\Theta,\Phi) \cos\Theta \, \partial\omega$$

Upwelling irradiance,

$$E_u = \int_{\Phi=0}^{2\pi} \int_{\Theta=\pi/2}^{\pi} L(\Theta,\Phi) \cos\Theta \, \partial\omega$$

where $\Theta = 0$ indicates the downward normal direction.

Absorption coefficient, a — The fraction of radiant energy absorbed from a collimated beam per unit distance ∂x.

$$a = \frac{-(\partial\Phi)_{abs}}{\Phi \partial x} \text{ in m}^{-1}$$

Scattering coefficient, b — The fraction of radiant energy scattered from a collimated beam per unit distance ∂x.

$$b = \frac{-(\partial\Phi)_{scat}}{\Phi \partial x} \text{ in m}^{-1}$$

Total attenuation coefficient, c — The fraction of radiant energy removed from a beam per unit distance ∂x owing to the combined processes of both absorption and scattering.

$$c = -\left[\frac{(\partial\Phi)_{abs} + (\partial\Phi)_{scat}}{\Phi \partial x}\right]$$

$$= a+b \qquad \text{in m}^{-1}$$

Scattering albedo, ω_o — The number of scattering interactions expressed as a fraction of the total number of interactions.

$$\omega_o = \frac{b}{c}$$

Volume scattering function, $\beta(\Theta)$ — The scattered radiant intensity in a direction Θ per unit scattering volume ∂V normalized to the incident irradiance E. Appropriate integrations of $\beta(\Theta)$ provide mathematical definitions of the scattering, forwardscattering and backscattering coefficients.

$$\beta(\Theta) = \frac{\partial I(\Theta)}{E \partial V} \text{ in m}^{-1} \text{ sr}^{-1}$$

Forwardscattering probability, F — The ratio of the scattering into the forward hemisphere (i.e., the hemisphere ahead of the interaction) to the total scattering into all directions.

$$F = \frac{\int_{\Phi=0}^{2\pi} \int_{\Theta=0}^{\pi/2} \beta(\Theta)\partial\omega}{\int_{\Phi=0}^{2\pi} \int_{\Theta=0}^{\pi} \beta(\Theta)\partial\omega}$$

Backscattering probability, B — The ratio of the scattering into the backward hemisphere (i.e., the hemisphere behind the interaction) to the total scattering into all directions.

$$B = \frac{\int_{\Phi=0}^{2\pi} \int_{\Theta=\pi/2}^{\pi} \beta(\Theta)\partial\omega}{\int_{\Phi=0}^{2\pi} \int_{\Theta=0}^{\pi} \beta(\Theta)\partial\omega}$$

Forwardscattering coefficient,

$$Fb = \int_{\Phi=0}^{2\pi} \int_{\Theta=0}^{\pi/2} \beta(\Theta)\partial\omega \quad \text{in } m^{-1}$$

Backscattering coefficient,

$$Bb = \int_{\Phi=0}^{2\pi} \int_{\Theta=\pi/2}^{\pi} \beta(\Theta)\partial\omega \quad \text{in } m^{-1}$$

Scattering coefficient,

$$b = \int_{\Phi=0}^{2\pi} \int_{\Theta=0}^{\pi} \beta(\Theta)\partial\omega \quad \text{in } m^{-1}$$

where $b = Fb + Bb$.

Volume reflectance (irradiance ratio, irradiance reflectance or diffuse reflectance), R — The ratio of the upwelling irradiance to the downwelling irradiance at any point.

$$R = \frac{E_u}{E_d}$$

Irradiance attenuation coefficient, K — The logarithmic depth derivative or the downwelling irradiance at depth z.

$$K(z) = \frac{1}{E_d(z)} \left[\frac{\partial E_d(z)}{\partial z} \right] \text{ in } m^{-1}$$

Scalar irradiance, E_0 — The integral overall directions of the radiance distribution at a point.

$$E_0 = \int_{\Phi=0}^{2\pi} \int_{\Theta=0}^{\pi} L(\Theta,\Phi)\partial\omega \quad \text{in W } m^{-2}$$

Downwelling scalar irradiance, E_{0d}

$$E_{0d} = \int_{\Phi=0}^{2\pi} \int_{\Theta=0}^{\pi/2} L(\Theta,\Phi)\partial\omega \quad \text{in W } m^{-2}$$

Downwelling distribution function, D_d — The ratio of the downwelling scalar irradiance at depth z to the downwelling irradiance at that depth.

$$D_d(z) = \frac{E_{0d}(z)}{E_d(z)}$$